UQAR

Université du Québec
à Rimouski

CONTRÔLE ENVIRONNEMENTAL DE LA STRUCTURE ET DE LA DISTRIBUTION DE LA COMMUNAUTÉ MICROBIENNE DANS LE GOLFE DE SAN JORGE, ARGENTINE

ENVIRONMENTAL CONTROL OF THE STRUCTURE AND DISTRIBUTION OF THE MICROBIAL COMMUNITY IN THE GULF OF SAN JORGE, ARGENTINA

Mémoire présentée

dans le cadre du programme de maîtrise en océanographie

en vue de l'obtention du grade de *maître* en science

PAR

© MAITÉ PILMAYQUEN LATORRE

Juin 2018

Composition du jury :

Michel Gosselin, président du jury, Université du Québec à Rimouski

Gustavo A. Ferreyra, directeur de recherche, Université du Québec à Rimouski,

CADIC

Irene R. Schloss, codirectrice de recherche, CADIC

Lemarchand, Karine, codirectrice de recherche, Université du Québec à Rimouski

Gaston Almandoz, codirecteur de recherche, Universidad Nacional de la Plata

CONICET

Michel Starr, examinateur externe, Institute Maurice-Lamontagne

iv

UNIVERSITÉ DU QUÉBEC À RIMOUSKI
Service de la bibliothèque

Avertissement

À ma mère Adriana Nill et à mon père Victor Latorre, qui m'ont semé la curiosité par la mer.

REMERCIEMENTS

J'aimerais remercier l'expérience que m'apporté vivre à Rimouski. Dans ce petit endroit j'ai d'abord rencontré la neige, puis la chaleur des gens qui y vivent.

Je voudrais surtout remercier l'État d'Argentine qui, par le biais du programme BEC.AR m'a attribué une bourse pour réaliser cette maîtrise. Ma gratitude va aussi aux institutions, à l'Université du Québec à Rimouski et à l'ISMER, qui ont cordialement reçus l'ensemble des boursiers Argentines, répondant à tous nos besoins, grâce à des bourses, des programmes d'apprentissage du français et tout le matériel nécessaire pour réaliser mon travail de recherche.

Je tiens à remercier tout particulièrement mes directeurs Gustavo Ferreyra, Irene Schloss, Karine Lemarchand et Gaston Almandoz pour m'avoir accompagné tout au long du processus, m'enseignant les techniques de traitement des données, m'aidant à interpréter les résultats et à écrire ce présent mémoire. Je voudrais également remercier Gustavo et Irene de m'avoir accueillie en famille, de m'avoir écouter et de m'avoir soutenir dans les moments les plus difficiles.

Je tiens à remercier "Les Filles", Juli, Xime, Elo et Ary, ce petit groupe d'Argentines rêveur et fort. Ça n'aurait pas été pareil sans vous. Merci pour les mates et les promenades au beau Québec.

Merci à mes colocs, qui ont été nombreux et chacun m'a donné de beaux souvenirs, de différentes histoires et la chaleur humaine pour me sentir comme chez moi. Pour Mymy, Jean et Arthur, j'espère que nous nous reverrons quelque part.

À Catty, Mary-Ann et Catty! Merci pour la belle « maison jeune », les fêtes et les randonnées à la plage.

A ma famille qui m'accompagne pendant tout le processus et m'encourager à suivre mes rêves.

AVANT-PROPOS

Le présent travail s'inscrit dans le cadre du projet "Santé de l'écosystème marin du golfe San Jorge: état actuel et résilience" (MARES, pour son acronyme en anglais), faisant partie du projet de coopération internationale entre l'Argentine et le Québec. Ce projet a pour but d'étudier l'état actuel de l'écosystème marin du golfe de San Jorge. C'est dans ce contexte que j'ai obtenu une bourse du programme BEC.AR (Argentine) pour suivre des études de maîtrise en océanographie à l'ISMER-UQAR. Au cours de l'année 2016 j'ai reçu de l'aide financière du Service aux Étudiantes de l'UQAR afin de participer à la mission océanographique du programme Pampa Azul dans le golfe San Jorge, en Argentine. Trois présentations des résultats préliminaires ont été effectuées pendant le développement de ma maîtrise, à l'intérieur des rencontres scientifiques suivants :

- Latorre, MP, Schloss I., Almandoz G., Lemarchand K., Ferreyra G. "Environmental controls of the microbial community structure and distribution in San Jorge Gulf, Argentine". Présentation des résultats de maîtrise. Mars 2017, Workshop PROMESse, Rimouski, Québec. Orale.

- Latorre, Maité G. Almandoz, K. Lemarchand, I.R. Schloss, G.A. Ferreyra, "Biomass distribution of the microbial community and evaluation of its physiological state in the San Jorge Gulf", . Novembre 2016, 15e Assemblée Générale Annuelle de Québec-Océan. Affiche.

- Latorre, M.; Schloss I.; Almandoz G. ; Lemarchand K. ; Ferreyra G., "Contrôle environnemental de la structure et de la distribution de la communauté microbienne dans le Golfe de San Jorge, Argentine", Novembre 2015. 14e Assemblée Générale Annuelle de Québec-Océan. Affiche.

RÉSUMÉ

Le golfe de San Jorge (GSJ) englobe un écosystème très productif de la Patagonie argentine. Dans ce contexte, la communauté microbienne joue un rôle essentiel en générant le carbone organique qui sera consommé dans le réseau trophique marin de cette région. L'objectif de cette étude était de caractériser la composition et biomasse de la communauté microbienne et l'état physiologique du composant autotrophe en relation aux facteurs environnementaux les plus importants. L'échantillonnage a été effectuée à 16 stations à bord du R/V Coriolis II de l'Université du Québec à Rimouski, en été. La structure verticale et les courants dans la colonne d'eau ont été mesurés et des analyses chemiques et la composition et biomasse de la communauté microbienne ont été effectués. Nos résultats montrent que la température (driver primaire de la stratification dans la colonne d'eau) et les nutriments affectent la composition et distribution de la communauté. En utilisant un estimateur de la stabilité dynamique (le nombre de Richardson), il a été possible de détecter des processus turbulents dans des zones stratifiées associé à la marée et au cisaillement des masses d'eau, lesquels ont favorisé la rupture de la pycnocline. De plus, la formation de doigts de sel a été favorisé pour l'entrée des eaux de faible salinité à l'extrême sud du GSJ. Ceci suggère que les deux processus contribuent au pompage des nutriments provenant des eaux profondes à l'interface de la pycnocline, lesquels favorisent le développement de micro-phytoplancton qui soutienne des réseaux trophiques herbivores. Cependant, la communauté était dominée par le pico-plancton qui constituent des réseaux du type boucle microbienne. Le phytoplancton a toujours montré des bonnes conditions physiologiques quant à leur capacité photosynthétique. Néanmoins, la biomasse de micro-phytoplancton était toujours faible (<3 µg l^{-1} de carbone). L'hypothèse que nous avons tiré pour expliquer cette apparente contradiction est que l'accumulation des grandes cellules autotrophes est contrôlée par le broutage, couplé avec un haut taux de renouvellement des autotrophes. Cette hypothèse peut aussi être soutenue si l'on considère les hauts rapports du carbone vs. azote (rapport C: N, en anglais), qui suggèrent la présence d'une forte activité de broutage du zooplancton.

Mots clés : Golfe de San Jorge, Communauté microbienne, Stabilité dynamique, Nombre de Richardson, doigts de sel, Gradient de nutriments, état physiologique du phytoplancton

ABSTRACT

The San Jorge Gulf (SJG), is a highly productive ecosystem in the Patagonia Argentina. This study characterizes the base of the food web, i.e. microbial community composition, biomass and physiological state in relation with environmental factors in the SJG during summer 2014. Samples were collected at 16 stations, onboard the oceanographic vessel of the Université du Québec à Rimouski *R/V Coriolis II,* for which vertical structure and currents were measured. Nutrients, chlorophyll-a, dissolved oxygen, the particulate organic carbon and nitrogen and the microbial community composition and biomass were studied. Our results show that temperature (which is the main driver of stratification of the water column) and nutrients affect the distribution of the microbial community. Using a dynamic stability estimator (the Richardson number), it was possible to detect turbulent processes in stratified zones, which favored the partial disruption of the pycnocline, related to tide energy and the shear between both surface and deep-water masses. In addition, *low salinity coastal waters* (LSCWs) in the southern part of the gulf induce instabilities associated with density that can favor the formation of salt fingers. We have hypothesized that both processes can be pumping nutrients from deeps waters to the surface promoting the micro-phytoplankton growing, which feed herbivorous food webs with high biomass production. However, the community was dominated by pico-plankton which leads to microbial food webs or microbial loops. Additionally, the physiological state related to photosynthetic capacity of autotrophs was good, nonetheless the micro-phytoplankton size biomass was not high (<3 µg l^{-1} of carbon). The hypothesis that we have drawn to explain this apparent contradiction is that the accumulation of large autotrophic cells is controlled by grazing, coupled with a high turnover rate of autotrophs. This can be supported by the high carbon vs. Nitrogen ratio (C: N ratio), which suggests the presence of a strong grazing activity by zooplankton.

Keywords: Gulf of San Jorge, Microbial community, Dynamic stability, Richardson number, Salt finger, Nutrient gradient, Physiological state of phytoplankton.

TABLE DES MATIÈRES

xiv

LISTE DES TABLEAUX

LISTE DES FIGURES

LISTE DES ABRÉVIATIONS, DES SIGLES ET DES ACRONYMES

Français

GSJ	Golfe de San Jorge.
CO_2	Dioxyde de carbone.
SW	Masses d'eau du plateau continental.
BMW	Masses d'eau de Beagle-Magellan.
Chl-*a*	Chlorophylle -*a*.
N	Fréquence de Brunt–Väisälä.
Ri	Richardson nombre.
Rp	Rapport du gradient de densité.
PSII	Photosystème II.
F_v/F_m	Maximum rendement quantique de la photochimique du PSII.

Anglais

SJG	San Jorge Gulf.
CO_2	Carbon dioxide.
SW	Shelf waters.
BMW	Beagle-Magellan waters.
LSCW	Low salinity coastal waters.
Chl-*a*	Chlorophyll-*a*.
N	Brunt–Väisälä frequency.
Ri	Richardson number.
Rp	Density ratio.

PSII   Photosystem II.

F_v/F_m   Maximum photochemical quantum yield.

Z_{eu}   Euphotic zone.

DINO   Dinoflagellates.

DIAT   Diatoms.

Nano-CYAN Nanocyanobacteria.

Nano-Euk Nanoeukaryotes.

Pico-CYAN Picocyanobacterial.

Pico-EUK Picoeukaryotes.

H-BACT   Heterotrophic free bacteria.

$\Delta N/\Delta z$ Nutrients gradient.

RDA   Redundancy analysis.

F_v/F_m   Maximum photochemical quantum yield.

POC   Particulate organic carbon.

PON   Particulate organic nitrogen.

C: N   Ratio between the organic carbon and nitrogen.

POC_{MC}   Particulate organic carbon of microbial community.

POC_A   Particulate organic carbon of autotrophs.

POC_H   Particulate organic carbon of heterotrophs.

POC_{MC}/POC_T Ratio between microbial community and total particulate organic carbon.

POC_A/ POC_H Ratio between autotrophs and heterotroph particulate organic carbon.

POC_H/ POC_T Ratio between heterotrophs and total particulate organic.

LISTE DES SYMBOLES

Français

σ_{PSII} Section efficace d'absorption du PSII.

σ_θ Density anomalies.

Anglais

σ_{PSII} Effective absorption cross section of PSII.

σ_θ Anomalies de densité.

INTRODUCTION GÉNÉRALE

PROBLÉMATIQUE

Quarante pourcents de la production primaire de la planète proviennent des écosystèmes océaniques (Falkowski, 1994). Les zones les plus productives sont concentrées dans les régions côtières, telles que la plate-forme de Patagonie argentine (située dans l'Atlantique sud-ouest) qui a été identifié comme l'un des écosystèmes marins les plus importants de l'hémisphère sud (Bisbal, 1995, Gregg et al., 2005). Elle présente une productivité primaire très élevée ($>300g$ m^2an^{-1}) (Behrenfeld et Falkowski, 1997), concentrée surtout près des zones frontales dans les talus et dans les différentes zones côtières (Acha et al., 2004).

Il n'existe cependant que peu de connaissances concernant la communauté microbienne qui soutient ces niveaux élevés de productivité. La richesse du golfe est reflétée par les images satellitaires qui montrent des concentrations élevées de chlorophylle-*a* (Chl-*a*) pendant le printemps et l'été (Glembocki et al., 2015). De plus, cette région du globe joue un rôle clé dans les cycles biogéochimiques globaux agissant comme un puits de CO_2 (Schloss et al., 2007); contribuant ainsi à atténuer les effets du changement climatique. Cependant, certaines zones proches de la côte peuvent également être des sources de CO_2 en période estivale (Bianchi et al., 2005), lorsque les conditions hydrographiques telles que la stratification limitent l'entrée des nutriments à la surface et donc l'accumulation de biomasse de phytoplancton. Il a été démontré que non seulement les variations dans la composition du phytoplancton affectent le bilan de CO_2, mais aussi que les réseaux trophiques microbiens affectent la productivité de cet écosystème (Schloss et al., 2007). L'étude des communautés microbiennes est donc fondamentale pour comprendre la productivité élevée de cet écosystème et son rôle de la région à l'échelle globale.

Situé dans la zone côtière de la Patagonie, le golfe de San Jorge (GSJ, 45-47 ° S et 65 ° 30 'O) représente une aire d'une grande richesse en termes de productivité et de biodiversité marine. Ce golfe est un bassin semi-ouvert d'une profondeur moyenne de ~100m, à l'exception d'un seuil (60m) à l'extrême sud-est qui s'étend en direction nord-est jusqu'à la moitié du Golfe (Louge et al., 2004). La zone est caractérisée par de faibles précipitations (229 mm an^{-1}), par l'absence de rivières et par la présence de vents prédominants d'ouest de 32,4 km h^{-1} en moyenne, atteignant des valeurs maximales de 73 km h^{-1} (Martin et al., 2016). Les propriétés hydrographiques montrent que les eaux du Golfe sont le résultat d'un mélange d'eaux provenant des eaux du plateau (salinité entre 33,4 et 33,8), et les eaux côtières provenant du canal Beagle et du détroit de Magellan (*Beagle-Magellan waters BMW*, en anglais), ayant une salinité inférieure à 33,4 (Bianchi et al., 2005, Fernandez et al., 2005). La circulation est dominée par des fortes marées, des vents d'ouest et des échanges de chaleur avec l'atmosphère (Tonini et al., 2006, Palma et al., 2008, Matano et al., 2010). La circulation moyenne est antihoraire, avec deux gyres intenses dans les extrêmes sud et nord, où le mélange provoque la formation de fronts qui définissent la frontière entre des eaux stratifiées et celles verticalement mélangées (Tonini et al., 2006, Palma et al., 2008). Ces zones sont associées à des concentrations élevées de Chl-*a* (Akselman, 1996, Glembocki et al., 2015). Cette zone est d'une grande importance pour le recrutement des poissons d'intérêt commercial (Fernandez et al., 2005, Fernández et al., 2008, Gongora et al., 2012) ainsi que pour l'alimentation des mammifères et des oiseaux marins (Yorio et al., 2001).

Dans le GSJ, plusieurs activités de protection et d'exploitation de l'environnement existent depuis près d'un siècle. L'activité pétrolière est l'une des plus importantes et se développe dans la région depuis le début du 20e siècle. Son impact sur les écosystèmes marins réside dans le transport maritime du pétrole brut vers les raffineries du nord de l'Argentine (Numerosky, 2004, Petrotecnia, 2004). Des études mettent en évidence une pollution chronique dans les ports les plus importants de la zone côtière du Golfe, à savoir les ports des villes de Comodoro Rivadavia et Caleta Olivia, (Commendatore et al., 2007). La pollution a également été affectée par des déversements aigus en les années 1985 et 2007.

La deuxième activité d'exploitation de grande importance économique locale et nationale est la pêche industrielle. Les principales espèces sont le merlu (*Merluccius hubbsi*) et la crevette (*Pleoticus muelleri*). Ils ont tous les deux des zones reproductrices dans le golfe et sont parmi les des stocks les plus importants du pays (Fernandez et al., 2005, Gongora et al., 2012). Par ailleurs, dans la zone nord du golfe, le premier parc marin a été créé ("Patagonia Austral"), avec plus de 100 km de côtes et 40 îles, en raison de l'importance dans la biodiversité marine et des processus océanographiques qui le soutiennent, ainsi que pour la valeur esthétique et paysagère de ce milieu (Yorio, 2009). Malgré la grande importance économique et écologique du GSJ, les connaissances sur les processus physico-chimiques et biologiques qui expliquent cette énorme productivité sont limitées.

En général, les recherches précédentes concernant le plancton dans le GSJ ont porté sur les composantes autotrophes (Akselman, 1996), sur les estimations de biomasse du phytoplancton au moyen de la Chl-*a* (Cucchi Colleoni et Carreto, 2001) ou de la détection d'algues toxiques (Krock et al., 2015), ainsi que sur les estimations de la productivité primaire lié à l'azote (Paparazzo et al., 2017). Cependant, peu de recherches portent sur les communautés microbiennes.

LA COMMUNAUTÉ MICROBIENNE

La productivité des écosystèmes pélagiques dépend non seulement de la présence des producteurs primaires, mais aussi de la composition (i.e. la diversité des espèces constituant la communauté) et de la structure (i.e. l'abondance des espèces dans la communauté) des communautés microbiennes. Les organismes unicellulaires composant ce type de communauté ont des tailles inférieures à 200 µm et comprennent des cellules procaryotes et eucaryotes (i.e. des bactéries, du phytoplancton et des protozoaires).

La communauté microbienne joue un rôle fondamental dans les cycles biogéochimiques, en régulant les flux de matière et d'énergie à travers des réseaux trophiques marins (Falkowski et al., 2004). Ce rôle est variable et dépend de la structure de taille de la communauté, ce qui conduit à différents types de réseaux trophiques pélagiques (Legendre

et Rassoulzadegan, 1995). D'une part, dans un milieu bien mélangé, avec des fortes concentrations en nutriments allochtones (nitrates), les réseaux trophiques classiques ou herbivores sont développés. Ceux-ci sont caractérisés par de grandes cellules phytoplanctoniques (par exemple des diatomées) broutées par le macrozooplancton qui soutient un écosystème à productivité élevée et ayant une forte capacité d'exportation du carbone organique vers les eaux profondes. D'autre part, lorsque les conditions environnementales sont stables (faible mélange vertical), les nutriments deviennent limitants et la reminéralisation bactérienne fournit de l'azote sous sa forme réduite (ammonium). Dans ces systèmes, les cellules de petite taille (pico-phytoplancton) sont favorisées. Ensuite, les réseaux trophiques qui se développent sont du type boucle microbienne (Azam et al., 1983), où le système se nourrit de la régénération de la matière organique (production régénérée) grâce à la reminéralisation des nutriments. Par conséquent, il y a une faible productivité de l'écosystème en termes de biomasse et peu ou pas de transfert de carbone organique vers les niveaux trophiques supérieurs. Pour ces raisons, l'étude de la composition et de la structure de taille des communautés planctoniques est essentielle pour comprendre le fonctionnement des écosystèmes pélagiques.

Dans les écosystèmes marins, la transformation de la matière et de l'énergie est gouvernée par une combinaison de facteurs physiques, chimiques et biologiques. L'analyse des communautés microbiennes a donc besoin d'une approche multidisciplinaire. Dans le GSJ, la documentation sur les communautés autotrophes concernent principalement le micro-phytoplancton (diatomées et dinoflagellés). L'étude la plus détaillée remonte à environ 30 ans, lors de la réalisation du doctorat d'Akselman (1996, données non publiées). Dans le GSJ, l'accumulation de la biomasse du phytoplancton, qui présente habituellement deux pics, l'un au printemps et l'autre à l'automne, est liée aux processus de formation et de rupture de la pycnocline (Akselman 1996). Comme dans d'autres écosystèmes marins tempérés, la période estivale est caractérisée par une forte stratification de la colonne d'eau, ce qui entraîne une limitation des nutriments dans la couche euphotique. Cependant, les observations par satellite effectuées entre 2000 et 2008 ont montré des niveaux élevés de chlorophylle-a (3 mg m^{-3}) pendant l'été autour de la zone côtière et à l'embouchure du golfe

(Glembocki et al., 2015). Dans ce contexte, il est important de déterminer si le GSJ pourrait être considéré, ou non, comme un système productif durant l'été en analysant la composition de la communauté et les conditions physiologiques de la composant autotrophe qui nous renseignent sur son potentiel productif.

ÉCHAPPER À LA BARRIÈRE DE LA STRATIFICATION : LES PROCESSUS DE MÉLANGE À LA PYCNOCLINE ET LEURS IMPORTANCE DANS L'APPORT DE NUTRIMENTS

Les conditions hydrodynamiques, la lumière et la disponibilité des nutriments sont les principaux facteurs influençant la composante autotrophe des communautés microbiennes (Margalef, 1978, Legendre et Rassoulzadegan, 1995, Cullen et al., 2002). Les vents, les marées et les ondes internes sont des mécanismes qui fournissent l'énergie nécessaire pour le processus de mélange vertical, et donc favorisent le renouvellement des nutriments dans les eaux de surface et sa productivité primaire. Dans les mers tempérées, le cycle de formation annuel de la pycnocline, dû au réchauffement des eaux de surface au printemps et en été, génère une barrière physique qui limite l'entrée des nutriments dès les eaux profondes vers les eaux de surface. Cependant, d'autres processus physiques tels que le mélange turbulent ou la double diffusion, peuvent aussi générer la rupture de la pycnocline permettant le renouvellement des nutriments dans la surface, nécessaire pour la photosynthèse (Thorpe, 2007).

Dans la colonne d'eau, le mélange généré par le mouvement des fluides à travers différentes isopycnes (couches de densité constante), est le "mélange diapycnal" (Thorpe, 2007). Le degré de stabilité de la colonne d'eau est lié aux changements de densité avec la profondeur (gradient de densité $d\rho / dz$). Si la densité ne change pas avec la profondeur, la stabilité est neutre ($d\rho / dz = 0$); Si la densité augmente avec la profondeur, la colonne d'eau est stable ($d\rho / dz > 0$) et au contraire, si la densité diminue avec la profondeur, la colonne d'eau est instable ($d\rho / dz < 0$). Le degré de stabilisation de la colonne d'eau peut être estimé à l'aide de la fréquence de Brunt–Väisälä (N). Ce terme exprime la capacité d'une particule à revenir à sa position initiale après avoir subi un petit déplacement vertical (Gill, 1982). La

formulation de cette stabilité statique prend en compte le gradient vertical de la densité et la force de la gravité. Les valeurs positives de N indiquent des conditions stables (Jackett and Mcdougall, 1995). À son tour, la profondeur du maximum valeur sert à positionner le maximum gradient de densité, marquant ainsi la position de la pycnocline. D'autre part, le nombre de Richardson (Ri) est un nombre sans dimension utilisé pour mesurer le gradient de densité dans un milieu stratifié stable avec écoulement de cisaillement (Galperin et al., 2007). Il représente le rapport entre la N^2 et le cisaillement. Parce qu'il incorpore un terme dynamique (le flux de cisaillement, mesuré comme le gradient de vitesse des masses d'eau), il est considéré comme un estimateur de la stabilité dynamique de la colonne d'eau. Si Ri est inférieur à 1, N^2 est négligeable. L'écoulement devient instable et turbulent en dessous la valeur théorique critique de Ri = 0,25. Cependant, une fois que le mélange a démarré, il peut continuer à des valeurs supérieures à 1. Pour cette raison, valeurs critiques entre 0,2 et 1 peuvent indiquer la présence de mélange turbulent (Galperin et al., 2007, Hans van Hare et al., 1999).

De plus, le processus de "double diffusion" a une origine différente du mélange turbulent. Pour qu'il se produise, la température et la salinité doivent diminuer avec la profondeur en provoquant des gradients positifs (Schmitt, 2003). Le déplacement vertical est généré sous la forme des intrusions d'eau salée (*salt fingers*) ascendants et descendants causés par des différences dans la diffusion moléculaire de la chaleur et de sel (Thorpe, 2007). Le rapport de densité Rp peut être utilisé pour détecter ce processus, en utilisant les valeurs de température et de salinité de la colonne d'eau et aussi que les coefficients d'expansion thermique et contraction haline (voir équation en Thorpe, 2007). La formation de doigts de sels est possible pour de valeurs de Rp entre 1 et 100 (Oschlies et al., 2003, Thorpe, 2007). Les deux types de mécanismes de mélange décrits ne se produisent pas simultanément. Le mélange turbulent est toujours plus important, cependant lorsque les conditions de cisaillement sont faibles, une double diffusion est possible et peut générer mélange (St. Laurent et Schmitt, 1998; Zhang et al., 1998). En termes quantitatifs, Ri doit être supérieur à 1 et 1 <Rp <3 (Thorpe, 2007). Pendant la saison estivale, lorsque les conditions de stratification sont fortes, la présence d'un processus ou de l'autre pourrait

amener des éléments nutritifs dans la zone euphotique et stimuler la production. Étant donné que les conditions environnementales à la formation de l'un ou de l'autre de ces processus sont favorables dans le golfe, nous proposons d'évaluer les deux et de tenter d'établir une relation avec le type de communauté microbienne présente. À ce jour, il n'y a aucune étude qui évalue des processus dans le GSJ. Ces processus pourront être clé afin d'évaluer le potentiel productif de la région en saison estivale.

L'ÉTAT PHYSIOLOGIQUE DU PHYTOPLANCTON ET LEUR RELATION AVEC L'ENVIRONNEMENT

Les conditions océanographiques exercent une pression sélective au niveau de la communauté autotrophe, affectant leur composition taxonomique, et au niveau cellulaire, provoquant des altérations tel que la quantité de pigments photosynthétiques qui entraînent des variations de la réponse physiologique (Moore et al., 2006, Litchman et Klausmeier, 2008). Les conditions de lumière, la turbulence ou la disponibilité des nutriments sont quelques-uns des facteurs les plus importants qui affectent l'efficacité de la photosynthèse (Litchman et Klausmeier 2008). L'état physiologique de l'appareil photosynthétique est généralement estimé à l'aide de mesures indirectes telles que l'émission de fluorescence (Maxwell et Johnson, 2000). Le concept sous-jacent dans ce type d'estimation est basé sur les processus qui ont lieu dans la cellule, spécifiquement dans le photosystème II (PSII). En bref, l'énergie lumineuse captée par la cellule peut suivre trois voies : être utilisée pour la photochimie, être dissipée sous forme de fluorescence ou être dissipée sous forme de chaleur (Maxwell et Johnson, 2000). Les trois processus sont en compétition les uns avec les autres, de telle sorte que l'augmentation de l'efficacité de l'un d'eux, provoque la diminution des autres. Certains des paramètres associés au photosystème II qui peuvent être dérivés des mesures de fluorescence, nous aide à évaluer l'efficacité de la photochimie et de la dissipation thermique (Maxwell et Johnson, 2000). Le deux le plus utilisé sont l'efficacité quantique maximale de la photochimique du PSII (F_v/F_m, en anglais *maximum photochemical quantum yield* of PSII, estimé comme le rapport entre la fluorescence variable et le maximum de fluorescence) et la section d'absorption efficace du PSII (σ_{PSII}, en anglais

effective absorption cross section of PSII). Ces deux paramètres ont une grande importance pour caractériser la réponse du phytoplancton aux changements environnementaux (Suggett et al., 2009).

Le paramètre F_v/F_m fait référence à la probabilité qu'un photon soit utilisé pour la photochimie en concurrence avec d'autres processus (Suggett et al., 2009). Des valeurs élevées de F_v/F_m indiquent de bonnes conditions physiologiques, atteignant un maximum de 0,65-1, diminuant dans des conditions de stress associées à une faible disponibilité en nutriments (Falkowski et Kolber, 1995). D'autre part, σ_{PSII}, est un estimateur de la proportion de lumière absorbée par l'antenne photosynthétique utilisable pour la photosynthèse (Maxwell et Johnson, 2000). Il est calculé comme le produit entre l'absorption de la lumière par la chlorophylle associée à l'antenne du PSII et la probabilité d'une réaction photochimique (Kolber et Falkowski, 1998, Moore et al., 2005). Au fur et mesure que la valeur σ_{PSII} augmente, l'efficacité de l'antenne photosynthétique augmente pour intercepter les photons (Moore et al., 2006). De cette façon, la variation de ce paramètre dépendra du type, de la concentration et de l'arrangement des pigments associés à l'antenne photosynthétique (Moore et al., 2006, Suggett et al., 2009). La composition des pigments dépend à son tour de l'espèce, mais elle est également affectée par les conditions de lumière et de la disponibilité de nutriments dans l'environnement. L'utilisation des deux paramètres pour évaluer la productivité des écosystèmes est de plus en plus répondue et l'état physiologique des communautés face à la limitation par nutriments (i.e., Greene et al., 1992, Kolber et al., 1998, Parkhill et al., 2001, Smyth et al., 2004, Yentsch et al., 2004, Moore et al., 2005, Fishwick et al., 2006, Suggett et al., 2009, Martin et al., 2010, Fujiki et al., 2014, Mino et al., 2014). Dans cette mémoire, il est proposé d'évaluer pour la première fois, l'état physiologique de la communauté phytoplanctonique en mer argentine, ce qui fournira des informations pertinentes pour comprendre la productivité des systèmes côtiers à haute productivité tel que le golfe San Jorge. De plus, puisque les deux paramètres étudiés sont liés à la composition taxonomique de la communauté, il est important d'interpréter ces valeurs en tenant compte en même temps la composition de la communauté et les conditions environnementales (Suggett et al., 2009).

OBJECTIFS ET HYPOTHÈSES

Le présent travail s'est développé dans le cadre du projet "Santé de l'écosystème marin du golfe San Jorge: état actuel et résilience" (MARES, pour son acronyme en anglais), faisant partie du projet de coopération internationale entre l'Argentine et le Canada, dans le but d'étudier l'état actuel de l'écosystème marin du golfe de San Jorge. Dans ce contexte, la présente étude vise à caractériser la variabilité spatiale de la communauté microbienne dans le golfe de San Jorge en lien avec les facteurs biologiques et environnementaux. Les objectifs spécifiques sont 1) d'évaluer les caractéristiques dynamiques de la colonne d'eau et son impact sur la dynamique des nutriments, 2) de décrire les modes de distribution de la communauté microbienne en fonction des variables environnementales, et 3) de déterminer l'état physiologique du phytoplancton à partir de paramètres photosynthétiques clés. Les hypothèses sont: a) Le mélange turbulents contrôlent l'entrée des nutriments à la surface dans les zones stratifies tandis que les intrusions de sel ne sont pas important dans la saison estivale b) La disponibilité des nutriments contrôle la composition et l'abondance de la communauté microbienne, c) Les communautés situées dans les zones frontales du golfe, avec un apport élevé en nutriments, ont un meilleur état physiologique exprimés à travers des valeurs plus élevées dans leurs paramètres photosynthétiques.

CHAPITRE 1

CONTRÔLE ENVIRONNEMENTAL DE LA STRUCTURE ET DE LA DISTRIBUTION DE LA COMMUNAUTÉ MICROBIENNE DANS LE GOLFE DE SAN JORGE, ARGENTINE

1.1 CONTEXTE DU PROJET

Cet article, intitulé « *Contrôle environnemental de la structure et de la distribution de la communauté microbienne dans le golfe San Jorge, Argentine* », a été rédigé avec mon directeur de maîtrise Gustavo Ferreyra et mes codirecteurs Irene Schloss, Gaston Almandoz et Karine Lemarchand. En tant que premier auteur, ma contribution à ce travail fut l'essentiel de la recherche sur l'état de l'art, le développement de la méthode, l'exécution des tests de performance et la rédaction de l'article. Le professeur Gustavo Ferreyra, a fourni l'idée originale. Il a contribué à la conception de cette recherche de pointe au développement des méthodes ainsi qu'à la révision de l'article. Mes codirecteurs Irene Schloss, Gaston Almandoz et Karine Lemarchand, ont aussi contribué à la conception de cette recherche, aux analyses des échantillons et des résultats, ainsi qu'à la révision de l'article. Une version abrégée de cet article sera présentée pour publication à l'éditeur de la revue scientifique *Oceanography* dans une édition spéciale sur le golfe San Jorge, à l'hiver 2018, dans le cadre du projet MARES-PROMESse.

1.2 **ENVIRONMENTAL CONTROL OF THE STRUCTURE AND DISTRIBUTION OF THE MICROBIAL COMMUNITY IN THE GULF OF SAN JORGE, ARGENTINE**

1.3 **INTRODUCTION**

The Argentine Patagonian shelf, located at the southwest Atlantic, has been identified as one of the most productive marine ecosystems in the southern hemisphere (Bisbal et al., 1995, Greeg et al., 2005). The San Jorge Gulf (SJG; 45-47° S and 65°30' W) is a shallow semi-open basin (~ 100 m deep), which supports a large fishery production (Fernandez et al., 2005, Gongora et al., 2012) and is an important breeding area for marine mammals and seabirds (Yorio et al., 2009). Westerly winds (~ 35 km h^{-1}, Martin et al., 2016), scarce precipitations (229 mm yr^{-1}) and no significant river inputs characterize this region. Hydrographic properties show that waters in the Gulf are the result of a mixture of shelf waters (SW; salinity ranging from 33.4 to 33.8) and coastal waters outflowing from the Beagle Channel and Magellan Strait (BMW; salinity < 33.4) (Bianchi et al., 2005, Fernandez et al., 2005). Different oceanographic models have shown that surface circulation is mainly driven by strong tides, western winds and exchanges of heat with the atmosphere (Tonini et al., 2006; Palma et al., 2008; Matano et al., 2010). The average circulation is counterclockwise, with two intense gyres in the south and north extremes, influenced by bottom topography (Tonini et al. 2006, Palma et al., 2008). Despite its great economic and ecological importance, the knowledge about the physical-chemical and biological processes that regulate its high productivity is limited.

The organisms that constitute the base of the pelagic food web, here referred to as the "microbial community", comprise cells smaller than 200 µm, and include prokaryotic and eukaryotic groups of organisms (i.e. bacteria, phytoplankton and protozoa). They are key players in the biogeochemical cycles, generating the organic carbon that will be consumed at upper trophic levels or exported to the bottom (Falkowski et al., 2004). The impact of the microbial community on the organic matter cycling is variable and depends on the community size structure, which leads to different types of pelagic food webs (Legendre and

Rassoulzadegan, 1995). Herbivorous food chains are favored in mixed environments, rich in nutrients. The dominant groups are large cells (i.e. diatoms), grazed by macrozooplankton. These systems have the capacity to sequester large quantities of carbon and export them in depth. On the other hand, closed trophic chains, called microbial loops (Azam et al, 1983), develop in dynamically stable zones, with little or no nutrient supplement. These communities survive thanks to the bacterial remineralization of organic nitrogen to ammonium allowing its use by phytoplankton cells. In these systems the organic matter is continuously recycled and therefore, little or no organic carbon is exported to deeper waters. The study of the composition and size structure of this community is essential to understand the functioning of pelagic ecosystems. In general, previous plankton research in the SJG focused on the autotrophic component of the community, particularly on phytoplankton composition (Akselman, 1996), biomass by means of chlorophyll-a (Chl-*a*) determination (Cucchi Colleoni and Carreto 2001), toxic algae (Krock et al., 2015) and satellite observations (Glembocki et al. 2015). By contrast, community-oriented investigations of the area are still lacking.

The structure of the microbial community is the result of a combination of physical, chemical and biological processes that act in a complex way in space and time. The most relevant controlling factors are nutrients availability, light conditions and stratification of the water column (Glibert, 2016). In the SJG, the accumulation of phytoplankton biomass, which usually presents two peaks in spring and fall, is intimately coupled with the processes of formation and rupture of the pycnocline (Akselman, 1996). As in other temperate ecosystems, the summer period is characterized by a high stratification of the water column, which leads to nutrient limitation in the euphotic zone. However, multiyear satellite observations (2000 to 2008) showed high levels of chlorophyll-*a* (Chl-*a*, mean of 3 mg m^{-3}) during summer across the coastal and the mouth zone of the SJG (Glembocki et al. 2015).

A strong vertical stratification of the water column acts as a barrier for the input of nutrients to the euphotic zone. However, two main mechanisms may act under such stable conditions promoting turbulence and diapycnal mixing (across-isopycnal) (Thorpe 2007).

One is the "turbulent mixing", resulting from shear between water masses that lay on top of each other and have different current speed and direction, causing internal wave breaking and, consequently, turbulence. The other is "double diffusion", that can occur when vertical gradients of temperature and salinity have the same sign (both positive), represented by a decrease of temperature and salinity with depth (Schmitt et al. 2001). The differences between the molecular diffusion of heat and salt provoke small changes in water column density, and this translates into ascending and descending parcels of water known as "salt fingers". Both mechanisms are usually in competition. Turbulent mixing is always more important but when the shear is weak, double diffusion is possible and determines the net buoyancy flux (Laurent and Schmitt 1998). In the summer season, when conditions of stratification are strong, the occurrence of either process could bring nutrients to the euphotic zone and stimulate production. To date, there are no studies that evaluate these processes in the SJG, which could be important to infer about the productive potential of the region in summer.

The potential for primary production can be additionally inferred from the information on the physiological state of the phytoplankton cells. When we consider the autotrophic component of the community, changes in the environment not only cause changes in the species composition (Margalef 1978, Glibert, 2016), but also generate responses at the cellular level that affect efficiency of photosynthesis (Litchman and Klausmeier, 2008). Fluorescence emission of the active chlorophyll can be used to estimate the photosynthetic parameters linked to the physiological state of cells (Suggett et al., 2009). Biophysical properties of photosystem II (PSII) such as the maximum photochemical quantum yield of PSII (estimated as the ratio between variable and maximum fluorescence, F_v/F_m) and effective absorption cross section of PSII (termed σ_{PSII}) can be used to characterize the physiological response of phytoplankton to environmental changes (Greene et al., 1992, Suggett et al., 2009). Previous studies on natural communities have shown that F_v/F_m is higher in nutrient-replete than in nutrient poor environments, and further correlated with higher primary productivity rates (Falkowski and Kolber, 1995). Additionally, both F_v/F_m and σ_{PSII} are related to the taxonomic composition of the phytoplankton assemblages, so that

for the interpretation of these values it is important to consider the community composition and the environmental conditions (Suggett et al., 2009).

In this context, it is important to determine if the SJG can be considered as a productive system during summer. To answer this question, it is essential to better understand the relevance of physical processes supplying nutrients to the surface and their relation with phytoplankton physiological condition and potential productivity in the SJG.

The **MAR**ine ecosystem health of the San Jorge Gulf: Present status and **RES**ilience (**MARES)** project allowed to collect original data on the SJG onboard R/V Coriolis II, during the austral summer 2014. In this context, the present study aims 1) to relate the distribution patterns of the microbial community to the environmental variables, 2) to evaluate the dynamic characteristics (and dynamic stability) of the water column and their impact on nutrients' dynamics in order to estimate their availability for phytoplankton production, and 3) to determine the physiological state of phytoplankton by measuring key photosynthetic parameters that could shed light on microbial productivity in the area.

1.4   MATERIALS AND METHODS

1.4.1   Sampling

Samples were collected during the austral summer 2014 (February-March) onboard of the Canadian research vessel *R/V* Coriolis II in the frame of the project **MAR**ine ecosystem health of the San Jorge Gulf: Present status and **RES**ilience project (**MARES)**. As part of leg 3 of the cruise, a grid of 16 sampling stations was sampled, covering most of the area of the gulf (Figure 1).

Conductivity, temperature and pressure (depth) profiles were measured at each station with a CTD-rosette system (Sea-Bird 9 plus) to characterize the water column structure. Additional sensors were attached to the system to measure photosynthetically available

radiation (PAR; Biospherical Li-Cor QCR), in vivo fluorescence (Wetlabs Eco-Afl/Fl) and dissolved oxygen (SBE43).

Water samples for chemical and biological analyses were collected from three depths (surface at 2 m of depth, Chl-*a* maximum and below the pycnocline at 10 m from the bottom) by means of 12L Niskin bottles attached to the rosette. This was completed only at eleven of the 16 stations due to adverse weather conditions, while profiling was performed in all stations and data of all probes recorded (see Figure 1).

Additionally, CTD cast were performed every 2 h during a 36 h period at a fixed station (FS) located in the center of the Gulf to record variations in water column structure. In this study, we will present information concerning physical aspects such as salinity, temperature and Chl-*a* concentration for this fixed station. Results on community composition and carbon fluxes from this station can be found in Massé-Beaulne (2017).
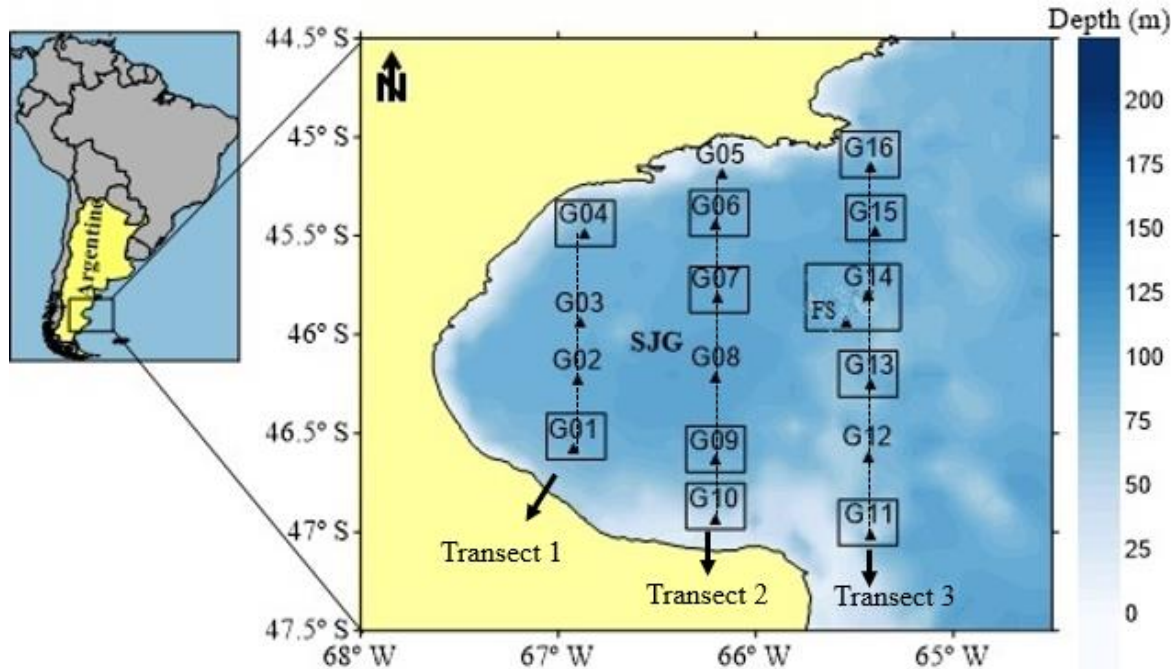
Figure 1: Study area in San Jorge Gulf (SJG). Triangles indicate location of CTD casts (G01 to G16 and FS). Doted lines indicate Transect 1, Transect 2 and Transect 3, respectively. Water (Niskin bottles) sampling stations are marked by squares (n=11).

1.4.2 Assessment of oceanographic conditions

The different water masses present in the Gulf were differentiated by means of a TS (temperature and salinity) diagram, according to the thermodynamic seawater equation (TEOS-10) using the package Gibbs-SeaWater (GSW) Oceanographic Toolbox (McDougall and Barker, 2011) with the Math Works MatLab R2014a program. Additionally, vertical CTD profiles were performed in three transects positioned in north-south direction parallel to the mouth of the Gulf (Figure 1). The interpolation was made using the kriging method in Surfer® 12.6.

The depth of the euphotic zone (Z_{eu}) was determined for each station and considered as the depth of the 1% of surface incident irradiance. It was calculated using the photosynthetic available radiation (PAR) data provided by the sensor and derived from Lamber-Beer law: $I_z = I_0 \exp(-k_d \Delta z)$, where I_0 is the ocean surface irradiance and k_d the diffuse attenuation coefficient estimated as the slope of the linear regression of irradiance at each station ($k_d = \frac{1}{\Delta z} \times \ln\left(\frac{I_0}{I}\right)$). Then, the Z_{eu} was calculated as (Mann and Lazier, 2006) :

$$Z_{eu} = \ln(0.01)/\text{k}d \qquad (1)$$

1.4.3 Water column stability

To assess water column stability and determine the position of the pycnocline, the Brunt-Väisälä buoyancy or frequency (N) was calculated with the following equation (Mann and Lazier, 2006):

$$N = \sqrt{(g|\rho)(\partial\rho|\partial z)} \qquad (2)$$

Where g is the gravitational acceleration (m s^{-2}), ρ is the mean seawater density (kg m^{-3}) and ($\partial\rho|\partial z$) is the vertical variation of density with depth. The N units are expressed in s^{-1}. The pycnocline was defined as the depth where the N was the highest.

To assess dynamic water column stability, turbulent mixing was estimated computing the Richardson number (Ri) and the diffusive mixing by the indirect measurement of the gradient of density (Rρ). Vertical profiles of currents were obtained with a narrowband 150 kHz acoustic Doppler current profiler (ADCP, RDI Ocean Surveyor) mounted at 3.9 m under the hull of ship. The data acquisition was done from 8 m depth to the bottom (~90 m) along the cruise. Raw data were recorded every 2 s. with a 4-m bins size. The values of horizontal velocity obtained were averaged within 4 s' intervals and corrected for errors due to the effect of shallowest depth, ship position and speed. The velocity values used in this work correspond to those recorded at each CTD station. Then, vertical shear was calculated as follow:

$$\left(\frac{\partial U}{\partial z}\right)^2 = \left(\frac{\Delta u}{\Delta z}\right)^2 + \left(\frac{\Delta v}{\Delta z}\right)^2 \tag{3}$$

Where $(\partial U/\partial z)^2$ is the square of the horizontal component of current, $(\Delta u/\Delta z)^2$ is the square of vertical gradient of horizontal E-W velocity and $(\Delta v/\Delta z)^2$ is the square of vertical gradient of horizontal N-S velocity, all expressed in m s^{-1} units. Then, the Richardson number was computed as:

$$Ri = \frac{N^2}{(\partial U/\partial z)^2} \tag{4}$$

The density ratio was calculated using:

$$R_\rho = \left(\alpha \frac{\partial T}{\partial z}\right) / \left(\beta \frac{\partial S}{\partial z}\right) \tag{5}$$

Where α and β are the thermal expansion and haline contraction coefficients, and $\frac{\partial T}{\partial z}$, $\frac{\partial S}{\partial z}$ are the vertical gradients of temperature and salinity, respectively.

1.4.4 Chemical analyses

The oxygen and fluorescence recorded with the rosette sensors were calibrated by the Winkler method (Aminot and Chaussepied, 1983) and the fluorimetric measure of Chl-*a* (see Section 1.4.5.1 below; Strickland and Parsons, 1981), respectively. Additionally, the percent of oxygen saturation (% O_2) was calculated according to Garcia and Gordon, (1992).

Seawater samples at the three different depths mentioned before were taken for inorganic nutrients determinations (nitrate+nitrite, phosphate and silicate) using a Skalar Autoanalyzer (Skalar Analytical 2005) at Centro Nacional Patagonico (CENPAT), Argentina.

For particulate organic carbon and nitrogen determinations (POC and PON), 500 ml samples were filtered onto Whatmann GF/F filters (pre-combusted at 450 °C, 5 h) and stored at -80°C in aluminum foil until analysis. Then, analyses were performed with a Continuous-flow Isotope Ratio Mass Spectrometry (CF-IRMS) using a Deltaplus XP mass spectrometer (ThermoScientific) coupled with an elemental analysis (EA) COSTECH 4010 (Costech Analytical).

1.4.5 Microbial community composition, abundance and biomass

1.4.5.1 Chlorophyll-*a*

For Chl-*a* analysis, 500 ml samples were filtered onto Whatmann GF/F filters and stored at -20°C in aluminum foil. Pigment extraction was made following Strickland and Parsons (1981) by immersion of the filters in acetone (90%) during 24 h in the dark at 4°C. Then, extracts were read before and after acidification with HCl (1 M) in a Turner 10 AU spectrofluorometer. Finally, Chl-*a* concentration was calculated following Strickland and Parsons (1981). Vertical profiles of Chl-*a* were obtained by calibration of the fluorescence (F) data from the rosette sensor with measured Chl-*a* data using a model I linear regression ([Chl-*a*] = 0.6139 x F + 0.2967, r^2 = 0.69, N = 38). The rosette was immersed at 4 m depth

for some minutes to allow the stabilization of the CTD, and the descent was at constant speed (0.5 m s^{-1}), after that fluorescence measures were made.

Samples at the Chl-*a* maximum were used for the identification and enumeration of microplankton, preserved in acid Lugol solution (final concentration 4%) and stored in 300 ml glass amber bottles at 4°C in the dark until microscopic analysis. For bacteria, pico- and nano-phytoplankton quantification, 5 ml samples were preserved with glutaraldehyde 25% (final concentration 0.5%) and stored at -80°C for further flow cytometry analysis.

Additionally, qualitative samples for microphytoplankton identification were collected with a 20 µm mesh net, preserved in acid Lugol solution (4%) and kept at 4°C in the dark until analysis. Taxonomic identification was done with a microscope Olympus BX51 following (Tomas, 1997).

1.4.5.2 Cell counts

Subsamples of 50 mL were settled for 24 h in a composite sedimentation chamber in order to count microplankton ($\geq$20 µm and $\leq$200 µm) following Utermöhl's method (1958), using a Zeiss Axiovert 100 inverted microscope. Cell dimensions of at least 10 specimens of each taxon identified were measured for biomass estimation. Cell biovolume (V) was calculated by assigning standard geometric shapes to each cells type identified (Hillebrand et al., 1999, Sun and Liu, 2003). Then, mean cell-specific biovolume was transformed into carbon content using different conversion factors for each group: pg C cell^{-1} = 0.288 V0.811 for diatoms (DIAT), pg C cell^{-1} = 0.216 V0.939 for other algal groups (Dinoflagellates, DINO) (Menden-Deuer and Lessard, 2000), pg C cell^{-1} = (lorica volume) x 0.553 + 444.5 for loricate ciliates (Verity & Langdon, 1984) and pg C cell^{-1} = 0.19 V µm^3 for aloricate ciliates (Putt & Stoecker, 1989) (CIL).

1.4.5.3   Flow cytometry analyses

Heterotrophic free bacteria and phytoplankton < 20 µm (i.e. pico- and nano-phytoplankton) were counted using an EPICS ALTRA flow cytometer (Beckman Coulter Inc.) equipped with a 488 nm argon laser (18 mW output), using 1 µm microspheres (Fluoresbrite YG, Polyscience) as internal standard to normalize cell size and fluorescence.

The protocol used for detection of heterotrophic free bacteria (H-BACT) is detailed in Belzile et al. (2008). Briefly, subsamples of 1 ml were stained with SYBR Green I (Invitrogen) in Tris-EDTA (1X) buffer to maintain a pH of 8. Bacteria were detected and enumerated in a cytogram of side scatter (SSC) vs. green fluorescence of nucleic acid-bound SYBR Green I at $\lambda = 530$ nm.

Cyanobacteria and eukaryotic phytoplankton were detected according to Tremblay et al. (2009). Samples were separated in subsamples of 1 ml, cyanobacteria were detected with orange fluorescence from phycoerythrin ($\lambda = 575$ nm) and phytoplankton with red fluorescence from chlorophyll-a ($\lambda = 675$ nm), both plotted versus forward side scatter (FSC). Pico-phytoplankton (Pico-EUK) and pico-cyanobacteria (Pico-CYAN) (between 0.2-2µm) and nano-phytoplankton/cyanobacteria (between 2-20 µm) were discriminated after size calibration with 2 µm polystyrene microspheres (Fluoresbrite YG, Polyscience). Cell concentrations were expressed in cell L^{-1}. The cytometric analyses were performed with Expo 32 v1.2b software (Beckman Coulter Inc.). For nanophytoplankton biomass calculation, forward scatter values were transformed into cell diameter using the calibration proposed by Belzile and Gosselin (2015). The carbon content of cells was calculated using different conversion factors and considering cells as spheres: 220 fg C m^{-3} for nano-phytoplakton (Tarran et al., 2006), 1.5 pg C $cell^{-1}$ for Pico-EUK, 12 fg C $cell^{-1}$ for H-BACT (Zubkov et al., 2000), 226 fg C $cell^{-1}$ for Pico-CYAN.

1.4.6 Physiological state of phytoplankton

The physiological state of phytoplankton assemblages was estimated by the fluorescence induction technique known as *Fast Repetition Rate fluorometry* (FRRF, Kolber et al., 1998) using a FRR fluorometer (FRRf; Chelsea Instruments, UK). Photosynthetic parameters were measured for water samples collected at the Chl-*a* maximum depth, using ten replicates for each station at 13 stations. Samples were exposed to dark conditions during 30 min to allow relaxation of fluorescence quenching and were then excited by an actinic light for measuring fluorescence emission according to Suggett et al. (2001). Photosynthetic parameters shown in this work are the maximum photochemical quantum yield of photosystem II (PSII), which is the ratio between the variable fluorescence ($F_v = F_v - F_m$) and the maximum fluorescence (F_m), and the effective absorption cross section (σ_{PSII}) of the PSII.

1.4.7 Statistical analyses

Statistical analyses were performed using RStudio© 2015. Regression analyses were used to determine relationships between related variables (e.g. Chl-*a* vs Fluorescence, Nitrate+nitrite vs phosphate). A Kruskal Wallis test was performed to compare photosynthetic parameters between stations, followed by a post-hoc Dunn test when differences were significant.

Relations between microbial community and environmental variables were evaluated with a canonical transformation-based redundancy analysis (tb-RDA) in RStudio© 2015 using vegan package (Oksanen et al., 2017). The Hellinger transformation was used to normalize the biomass matrix and minimize the effect of zeros (Legendre and Legendre, 1998, Legendre and Gallagher, 2001). This matrix included six groups: Pico-CYAN, Pico-EUK, H-BACT, CIL, DINO and DIAT. Nano-cyanobacteria/eukaryotes were not considered for the analysis to avoid the lack of normality due to their low biomass. The linearity and co-linearity of the environmental matrix were assessed with transformation (log x+1) and using the variance inflation factors (VIF) according to Zuur et al. (2010), respectively. The

explanatory variables with VIF>10 removed from the analysis. Seven remaining variables: N, Ri, temperature, salinity, oxygen, nitrate+nitrites and $\Delta N/\Delta z$ were used for the analysis. When the global model obtained by the RDA was significant (p<0.1), a forward selection of the significantly environmental was made by a stepwise selection of explanatory variables by permutation tests, and the Akaike Information Criterion (AIC) (Blanchet et al., 2014, Oksanen et al., 2017). Finally, a tb-RDA with retained environmental variables was conducted and assessed using the Monte Carlo permutation test.

1.5   RESULTS

1.5.1   General oceanographic conditions

The water mass characteristics are represented in the Temperature-Salinity diagram shown at Figure 2. The deepest waters, with density anomalies (σ_θ) > 25.8 kg m^{-3}, presented relatively homogenous thermohaline conditions, with low temperatures (~ 8º C) and high salinity (>33.4). Conversely, surface waters masses with σ_θ< 25.8 kg m^{-3} had heterogeneous thermohaline conditions and could be separated in two branches: a low salinity coastal water (LSCW), separated from shelf waters (SW) by the isohaline of 33.4. Between these two water masses surface temperature ranged between 13º C and 15º C, with the lowest values corresponding to the southern zone, where LSCW enters to the gulf.
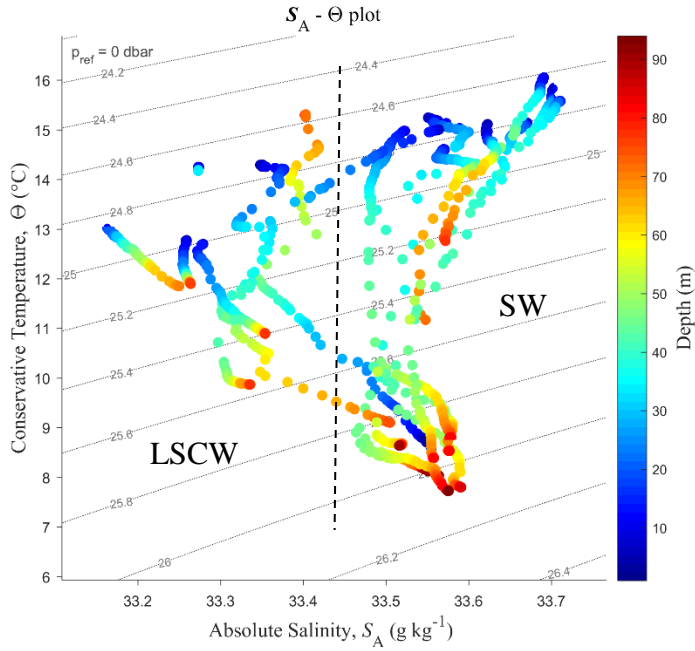
Figure 2: Temperature-Salinity diagram showing the characteristics of the different water masses from CTD casts for all stations at SJG during summer 2014. LSCW: Low salinity coastal waters, SW: Shelf waters.

To further explore the water column characteristics, three profile contours (in transects shown in Figure 1) of temperature, salinity and Brunt–Väisälä buoyancy are shown. Since density is highly temperature-dependent in this region, contour plots of density are not displayed because their shape is similar to that of temperature. The vertical profiles of temperature revealed a decreasing water temperature with depth (Figure 3a). In the inner stations (Transect 1 and 2), this trend was more marked leading to the establishment of a thermocline between 40-50 m depth. In the northern region, the thermocline was deeper, reaching 60 m depth (Station G05, G16). On the contrary, in the southeast zone the water column temperature was completely homogeneous, with intermediate temperatures (10-13º C, Section 3). Regarding salinity profiles, relatively constant conditions were found in the inner gulf, with salinity higher than 33.4 corresponding to SW and a smooth increase at surface until 33.5. A salinity decline was noticed in the southern zone (Transect 3), where the presence of a salinity minimum (33.1) defines the input of LSCW (G13, G12 and G11

stations) (Figure 3b). A remnant signal of this water mass was detected as a wedge at the pycnocline depth in the inner Gulf (Transect 2 at 40 m of depth).

Static stability, as measured by means of the Brunt–Väisälä frequency (N), showed high values at 40 m depth, corresponding to the pycnocline depth (Figure 3c). Comparing among stations, we found the lowest values at the southern zone (G09-G13), coinciding with the presence of weak or no stratification as we could observe in the temperature profiles. In all daytime stations where PAR could be recorded, the euphotic zone depth (Z_{eu}) coincided with the pycnocline (white lines, Figure 3c). Yet, at the stations where there was a weak stratification Z_{eu} was shallower (20 m of depth).

A detailed view of three typical vertical CTD profiles is displayed to show the prevailing conditions in the SJG (Figure 4). In addition to the CTD data, the vertical profile of Chl-*a* was added, which will be analyzed in detail in the next sections. Note the variation of salinity with depth, with the wedge of low salinity present at the central station (G07).

1.5.2   Dynamic stability conditions

Dynamic instability at the pycnocline was assessed in terms of turbulent motion, with the Richardson number, and in terms of convection (salt fingering), using the ratio of density, in order to understand the contribution of both of these mechanisms. Conditions of instability were assumed when Ri was < 1. In 60% of the cases Ri was >1 in the inner gulf. Ri<1 numbers were associated to the southern zone and one coastal station (G02) (ANNEXE 1). R_p was positive in 66% of the stations, showing the same sign (+) of the gradient of temperature and salinity with depth. Nevertheless, to stimulate convective processes that generate instability, both the density ratio must be $1<R_p<3$ and the condition of weak shear (Ri>1) must be present, which was not the case during the present work (ANNEXE 2).
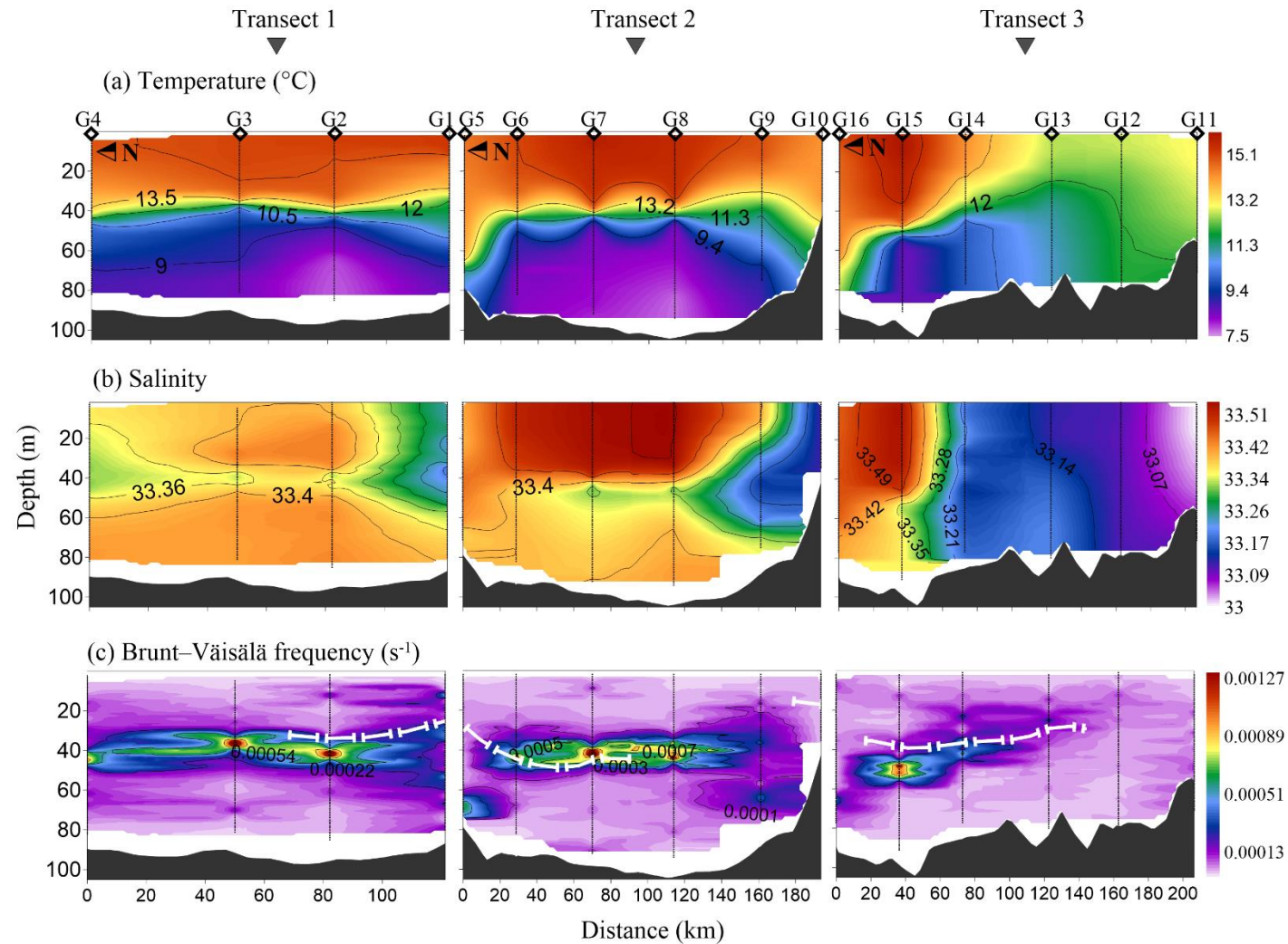
Figure 3: Vertical profiles of a) Temperature (°C), b) Salinity and c) Brunt–Väisälä frequency (s^{-1}) in the three transects studied (Transect 1: inner gulf; Transect 2: middle gulf; Transect 3: outer gulf). White lines indicate Z_{eu}.
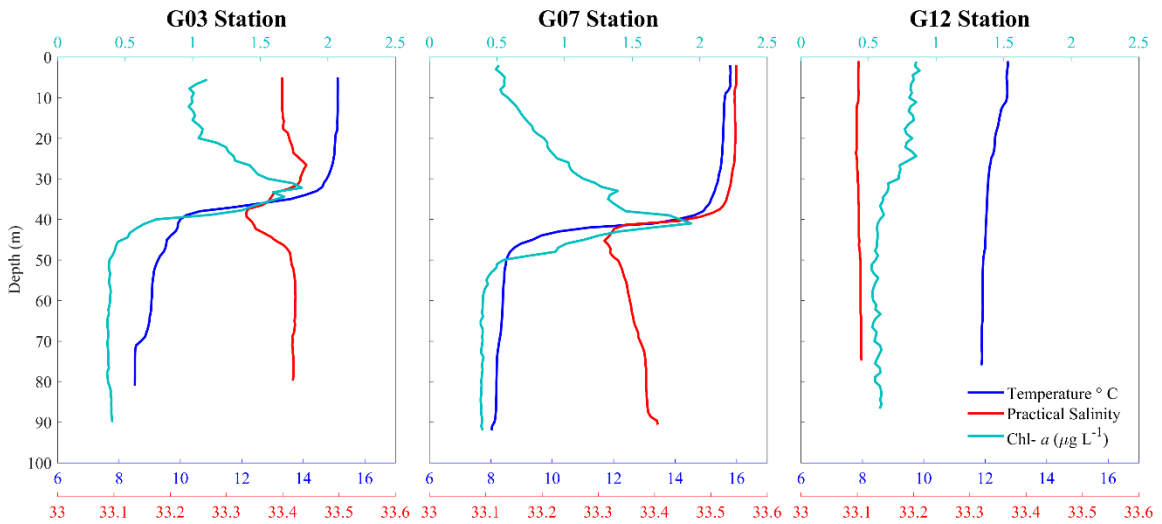
Figure 4: Vertical profiles of Temperature (º C, blue), Practical salinity (red) and Chl-*a* (µg L^{-1}, green) at three stations (G03, G07 and G13) in the SJG.

1.5.3 Nutrients distribution

Nitrate+nitrite concentrations ranged from non-detectable to ˜ 16.83 µM (Figure 5). In the southeastern zone, the concentration was vertically uniform in the water column with an average of ~6 µM. In the inner gulf, nutrients were almost depleted at surface and increased sharply in deep waters, where the highest concentrations were found. The presence of a nutricline was recorded between 40-50m, overlapped or under the pycnocline (Figure 5a). In general, phosphate concentrations ranged between 0.51-1.23 µM showing the same pattern than nitrates+nitrites, with lower concentrations in surface and increasing below the pycnocline (Figure 5b). Finally, silicate concentrations ranged between 0.59-6.12 µM with higher values below the pycnocline. In the inner gulf, the upper layer showed higher values reaching to 6 µM at surface in G07 station. The lowest concentrations were recorded in the southeast area (~0.9 µM) being homogeneous in the water column, and next to the coast at stations G03 and G04 (Figure 5c). The N:P and Si:N ratios were lower and higher than the

respective Redfield ratios (9.55 ±0.44; 1.81±0.17), with nitrates being the limiting nutrient especially in the surface layer (ANNEXE 3).
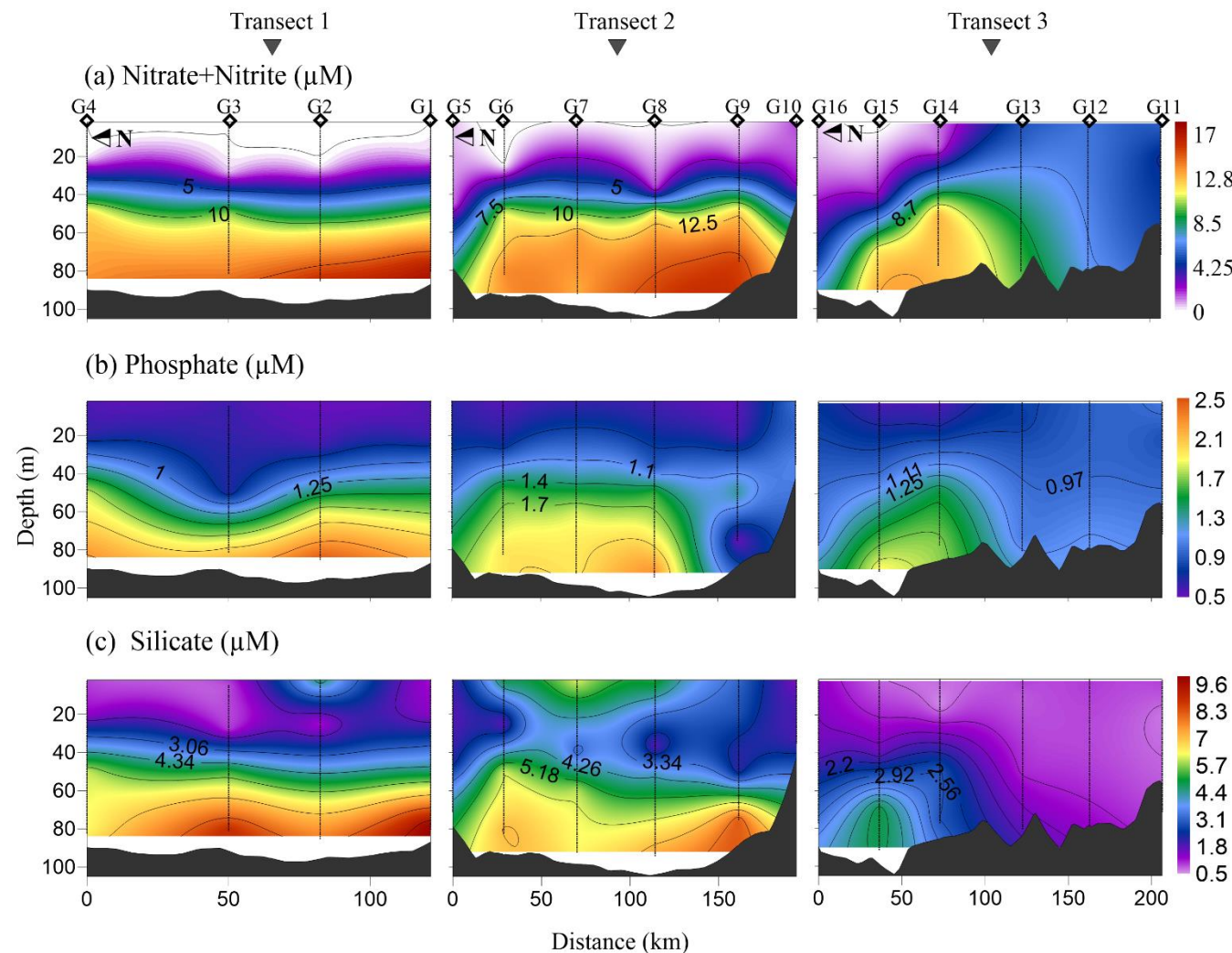
Figure 5: Vertical profiles of nutrients in the three transects studied (Transect 1: inner gulf; Transect 2: middle gulf; Transect 3: outer gulf).

1.5.4 Water column properties during the time series observations

The time series of temperature, salinity and Chl-*a* are shown in Figure 6 a, b and c, respectively. Note that the white rectangles indicate the lack of information for the station 5, which was not sampled, and between stations 7 and 8 because the time interval was greater than two hours. In Figure 6 d the horizontal current velocity averaged in Surface waters (0-40m of depth) and in Bottom Waters (40m to the bottom) was plotted. No variations in surface layer temperature and salinity were observed, although the depth of the thermocline varied between low tide (LT, 1, 2, 3) and high tide (HT, 4, 6), from 46 m to 32 m (Figure 6a and b). By contrast, both variables changed below the pycnocline. Salinity profiles show how LSCW entered the Gulf below the pycnocline during the tide rise (stations 4, 6, 8, 12, 14), and outflowed at low tide (Figure 6 b). Chl-*a* was accumulated during the ebb tide, it was lower and around the mean 1.03 µg L^{-1} of the Gulf (See Section 1.5.6), being detected in the euphotic zone.

1.5.5 Vertical advection of nutrients associated to dynamical stability

As nitrate+nitrite were the limiting nutrients we evaluated the mechanisms of injection of these nutrients from deeper waters through the pycnocline. To do so, we calculated the nitrate gradient between the surface and below the pycnocline ($\Delta N/\Delta z$) and then plotted it as a function of Ri. We assumed that if Ri <1, turbulent processes can break the pycnocline and supply nutrients to the surface. Although Ri was >1 in most cases, an exponential decline of the nitrate gradient was observed with the decrease of Ri (r^2=0.5, Figure 7a), suggesting a pumping of this nutrient towards surface waters. Moreover, in the fixed station the trend was the same but in this case the instability was more evident, with lower values of Ri, following the tide cycle (r^2=0.8, Figure 7b; SF12 was eliminated from the regression because it was an outlier).
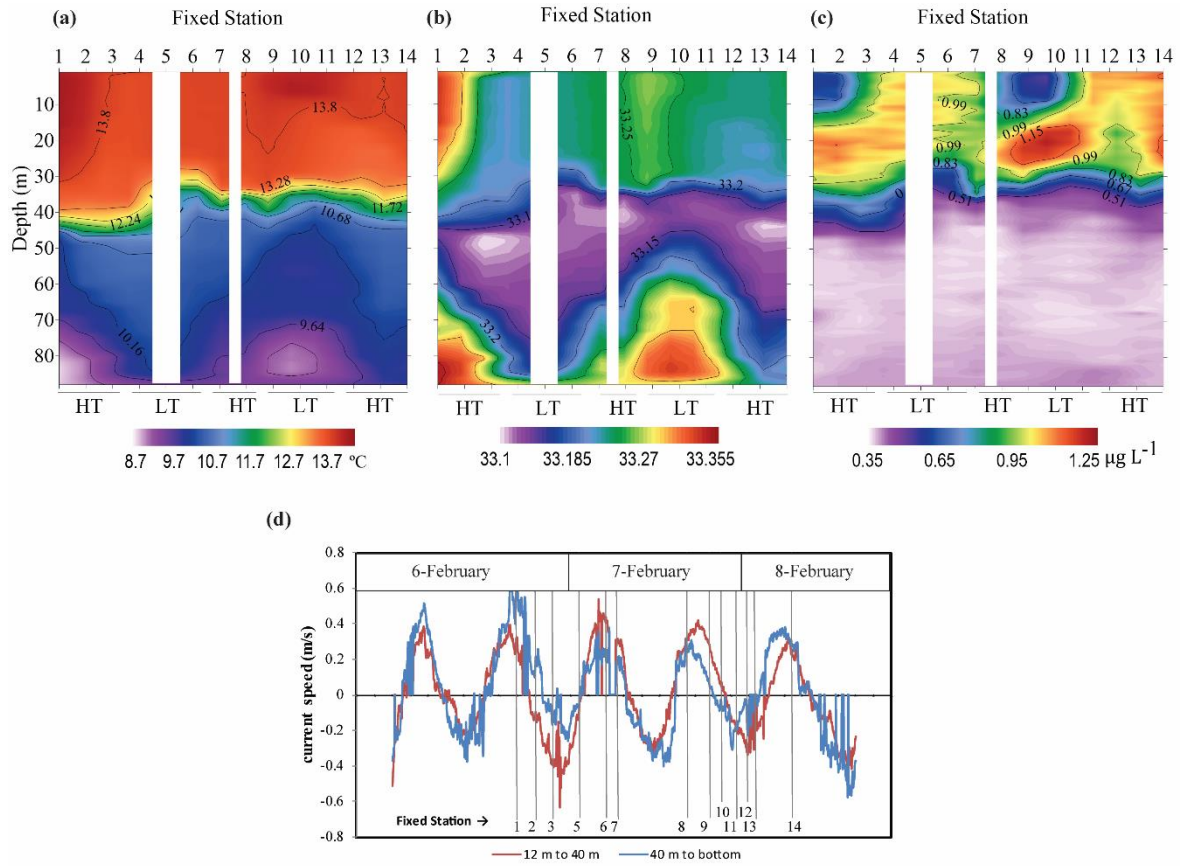
Figure 6: Time series at the Fixed station of a) Temperature (ºC); b) Salinity; c) Chlorophyll-a (µg L-1). Top x axes have the number of each CTD cast and bottom x axes the tidal cycle stage, where LT: Low tide; HT: High tide. White rectangles indicate the lack of data; d) Horizontal current velocity averaged in Surface waters (0-40m of depth) and in Bottom Waters (40m to the bottom). Doted lines correspond to each CTD cast.

(a)

$\Delta N/\Delta z= 0.1039\ln(Ri) + 0.1346$
$r^2 = 0.5095$

(b)

$\Delta N/\Delta z = 0.2075\ln(Ri) + 0.2658$
$r^2 = 0.8086$
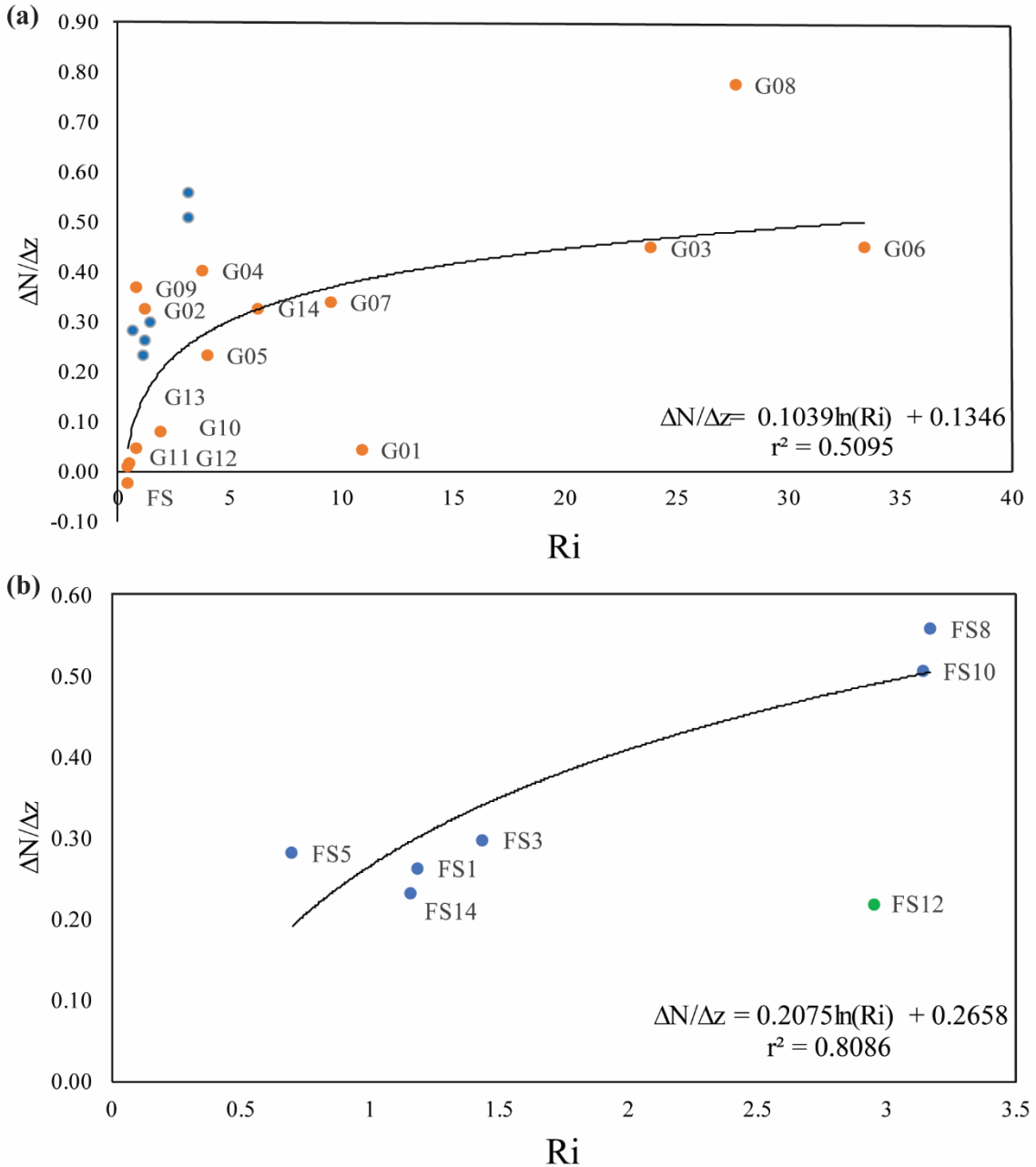
Figure 7: Gradient of nutrients (nitrates+nitrites) ($\Delta N/\Delta z$) *vs* Richardson number (Ri) at a) Grid stations (orange dots) and fixed stations (blue dots); b) Fixed station. The dotted line shows the logarithmic relationship between both variables.

1.5.6   Chl-*a* distribution associated to oxygen concentration

Maximum Chl-*a* concentrations were found at 20m at the coastal stations G01, G02 and G03, and at 40m at center stations G07, G08 and G09, always within the upper layer (above the pycnocline) (Figure 8a). The station G13 was the exception, in which high Chl- *a* values were uniformly distributed from the surface to 23m depth. The average concentration for the Gulf was 1.03 µg L^{-1} and the maximum values were always >2 µg L^{-1}, being highest at the coastal stations G01 (2.67 µg L^{-1}), in the western side of the Gulf. Dissolved oxygen was always >5 ml L^{-1} at the euphotic zone with three maximum values at stations G01, G09 and G03, in coincidence with high Chl-*a* values. Oxygen concentrations decrease with depth to minimal concentrations of 3.08 ml L^{-1}. However, in Transect 3 higher (>6 ml L^{-1}) concentrations were found in all the water column (Figure 8b). Regarding the percent of oxygen saturation (%O$_2$), this varied between 50-120%, having supersaturation of oxygen at the upper layer, with maximum values at station G01 and G13 (Figure 8c).
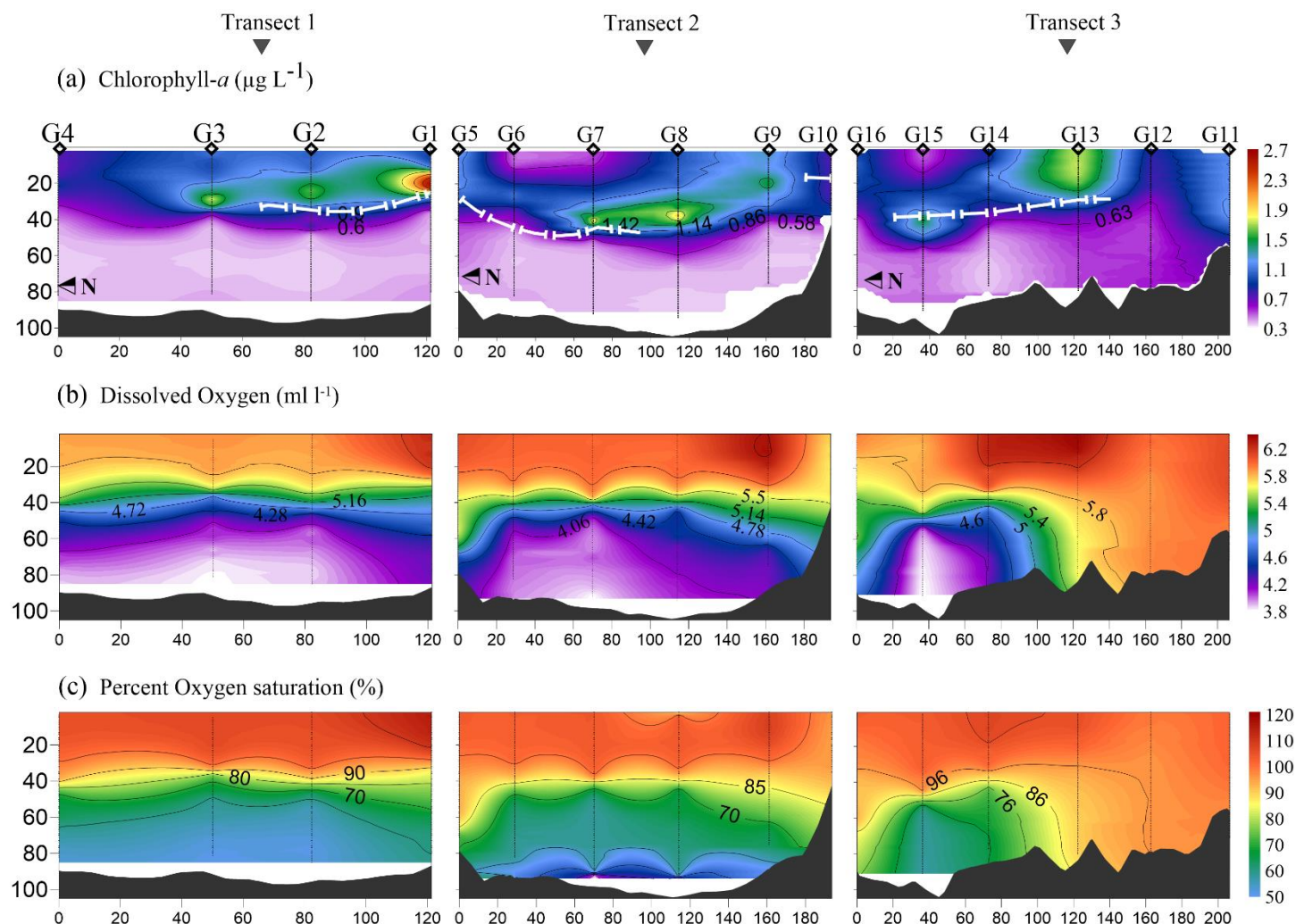
Figure 8: Vertical profiles of: a) Chl-*a* (µg L^{-1}), white lines indicate Z$_{eu}$;; b) Dissolved Oxygen (ml L^{-1}) c) Percent oxygen saturation (%) in three sections of the SJG (Transect 1: inner gulf; Transect 2: middle gulf; Transect 3: outer gulf).

1.5.7 Microbial community composition and biomass

The contribution of the different microbial community components was differentiated by size class (i.e. picoplankton, nanoplankton and microplankton, Table 1). Picoplankton dominated in the area, whose densities (cells L^{-1}) exceeded 3 to 4 orders of magnitude the microplankton and between 1-3 the nanoplankton. H-BACT showed the highest abundances, with a mean density of 1.5×10^9 cells L^{-1}. Within nanoplankton, the nano-cyanobacteria were usually the most abundant group, with average density of 1.2×10^5 cells L^{-1}. Regarding the microplankton, the diatoms showed the highest mean densities (3782 cells L^{-1}), followed by the ciliates (1861 cells L^{-1}) and the dinoflagellates (1351 cells L^{-1}).

Table 1 : Density (cells L^{-1}) of the main plankton groups classified by their size. Abbreviations means: Nano-CYAN: nanocyanobacteria, Nano-Euk: nanoeukaryotes, Pico-CYAN: picocyanobacterial, Pico-EUK: picoeukaryotes, H-BACT: heterotrophic bacteria.

						Station					
Group	G01	G04	G06	G07	G09	G10	G11	G13	G14	G15	G16
PICOPLANKTON											
Pico-CYAN	1.25×10^8	2.29×10^7	1.40×10^7	5.92×10^7	4.14×10^7	4.17×10^6	1.75×10^7	1.78×10^7	1.44×10^8	2.37×10^7	1.47×10^7
Pico-EUK	4.29×10^7	3.67×10^6	4.17×10^6	9.20×10^6	1.51×10^7	5.87×10^6	2.87×10^7	7.23×10^7	2.16×10^8	7.34×10^6	4.87×10^6
H-BACT	2.93×10^9	7.88×10^8	6.03×10^8	1.57×10^9	1.56×10^9	1.17×10^9	1.72×10^9	2.32×10^9	2.41×10^9	9.09×10^8	8.99×10^8
NANOPLANKTON											
Nano-CYAN	499412	6557	12247	5271	14045	0	0	333828	234604	176416	75440
Nano-EUK	7885	2459	0	3853	4115	2358	3199	4837	1804	2878	2070
MICROPLANKTON											
DINOFLAGELLATES	1600	356.3636	0	1380.909	1400	320	2100	1247.273	2620	3840	0
CILIATES	8000	5880	940	490	1100	680	420	178	620	1340	820
DIATOMS	1600	1069.091	120	0	340	80	13212.25	13616	20	80	11460

Analyzing each size class separately, pico-eukaryotes accounted for over 30% of total picoplankton carbon content in all stations (5.4-108.4 µg C L^{-1}), with maximum values in stations G01 (64.4 µg C L^{-1}) and G13 (108.3 µg C L^{-1}). Pico-cyanobacteria carbon content ranged between 2-35.6 µg C L^{-1}, with highest concentrations recorded at G01 and G14 (31.2 and 35.9 µg C L^{-1}, respectively). Heterotrophic bacteria carbon content varied between 7.2 and 35.5 µg C L^{-1}, reaching up to 35.2 and 28.9 µg C L^{-1} at G01 and G14 stations, respectively (Figure 9a, b and c).

In the microplankton size class, CIL were uniformly distributed in the Gulf with values between 0.9 and 12.9 µg C L^{-1}. DIAT (0-24 µg C L^{-1}) were mostly observed in the southern area. DINO were observed at the mouth of the Gulf, mainly in the northern zone, with values ranging from 0 to 23 µg C L^{-1} (Figure 9d, e and f). Nanophytoplankton was excluded from the results because their total carbon contribution was negligible (0.003 to 0.2 µg C L^{-1}) compared to the other groups.
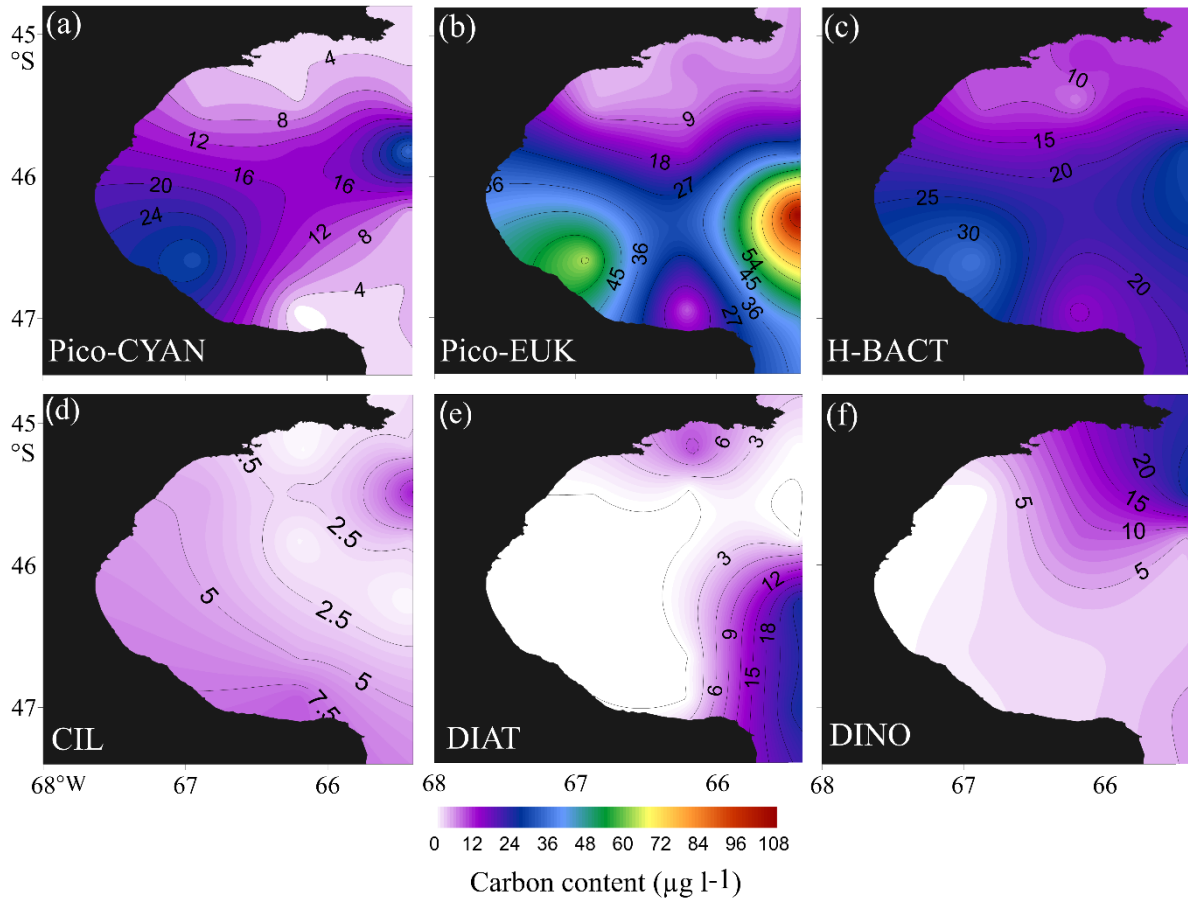
Figure 9: Horizontal distribution of carbon content (µg L^{-1}) of microbial community at Chl-*a* maximal depth. a) Pico-cyanobacteria; b) Pico-Eukaryotes; c) Heterotrophic bacteria; d) Ciliates; e) Diatoms, and f) Dinoflagellates.

Considering the relative contribution of each size class to the total microbial community biomass (autotrophs and heterotrophs), picoplankton accounted for 51% to 98% of total carbon microbial content (Figure 10). In terms of total carbon content, picoplankton dominated in the region with 2 to 6-fold higher concentrations at G01 and G13 compared with the other stations. The microplankton contribution was more variable (5%-48%), with the highest value in the northern zone at G15 station, while nanoplankton represented only a small fraction of total microbial carbon content (<0.6 %).
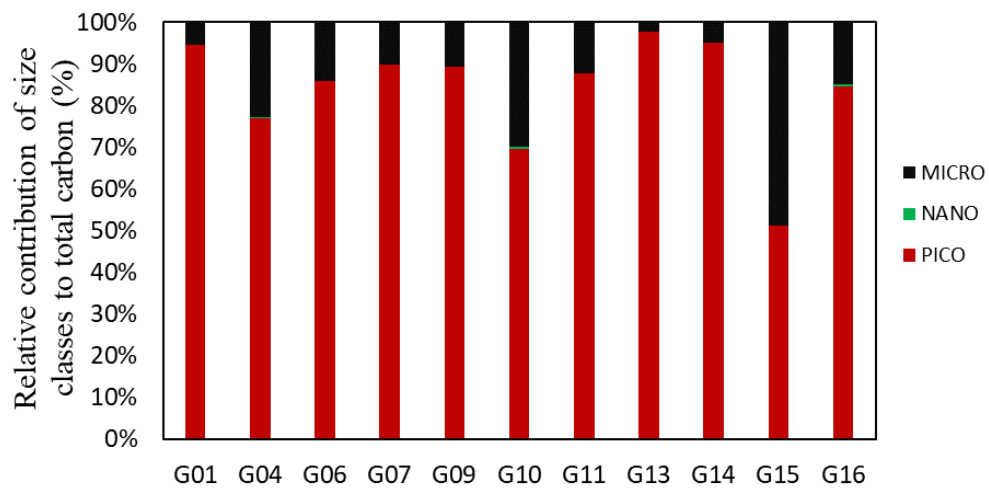
Figure 10: Relative contribution of each size class to total carbon content of the microbial community (%). MICRO: Microplankton, NANO: Nanoplankton, PICO: Picoplankton.

1.5.8 Multivariable analyses

The result of tb-RDA between environmental variables and the microbial community was significant ($p \ll 0.01$) explaining 52% (adjusted R^2) of the variance in the microbial community. The relationship between microbial community and environmental variables was illustrated in the correlation tb-RDA triplot (Figure 11). The proportion of variability explained by each canonical axis was expressed by the eigenvalues (λ). Together, the first two axes explained 51% of the variance, being $\lambda = 1.64$ and $\lambda = 0.81$, for the RDA1 (horizontal axis) and the RDA2 (vertical axis), respectively. The first axis was strongly correlated with

temperature. The second axis was closely influenced by the Richardson number and negatively correlated with nitrates+nitrites concentrations. The strength of the correlations between any pair of variables was represented by the angle between them. Moreover, the length of the lines expresses how representative was each taxonomic group. Pico-EUK was the best represented group in the Gulf, dominating the community at lower temperatures, being associated with relatively higher concentrations of nitrate+nitrite. At the opposite direction, H-BACT dominated at higher temperature and lower nutrient concentrations. Pico-CYAN was strongly correlated with waters having higher dynamical stability (Ri), low nutrients and relatively higher temperature. This group was closely associated with the presence of H-BACT. DIAT and DINO were related to low Ri and high nutrient availability. Finally, CIL were associated whit relatively higher temperatures, showing relatively high association with bacteria.

Regarding the input of stations distributions of the tb-RDA, it was clear the dominance of microplankton (DIAT, DINO and CIL) in the northern zone, and the pico-EUK at the southern east zone. The rest of the Gulf was dominated by a combination of different groups, with the southwestern area by pico-EUK/CYAN and the central zone (composed by the center and mouth of the gulf) by an assemblage of pico-CYAN and H-BACT, respectively.
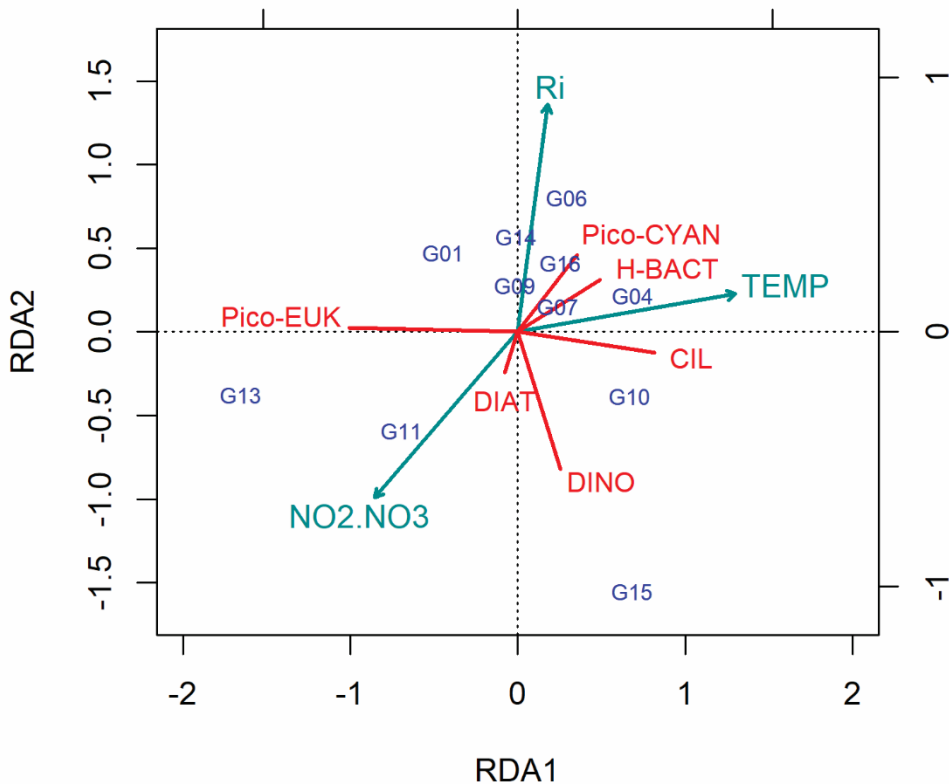
Figure 11: Canonical transformation-based redundancy analysis (tb-RDA) triplot of microbial community represented in terms of carbon content (μg L^{-1}) (red) and environmental variables (green) with samples in blue. The two first axes represent the 27% (RDA1) and 17% (RDA2) of total community variability.

1.5.9   Chl-*a* integrated to the upper layer and physiological state of the autotrophic community

Chl-*a* in the water column was integrated from surface to the pycnocline depth, since it coincided with the depth of the euphotic layer. This allowed the spatial distribution of the results from the sampled stations (Figure 12a). Values were over 40 mg m^{-2} in the whole Gulf, showing a marked accumulation in the southern zone, with a maximum of 85.5 mg m^{-2}

at a coastal station (G01) and other high values detected at G11 (67.91 mg m^{-2}) and G13 (63.97 mg m^{-2}).

The physiological state of the autotrophic assemblage was evaluated in terms of F_v/F_m and σ_{PSII} using an average of the ten measures taken at each station at the Chl-a maximal depth and then interpolating the results spatially. Both parameters showed significant differences between stations (Kruskal Wallis test, $p<0.05$). The maximum photochemical quantum yield of PSII varied from 0.29 in the coastal zone (G01) to 0.52 at the mouth of the gulf in northern and southern stations (Figure 12b). The central and southern coastal regions presented the lowest values compared to the rest of the Gulf, and these differences were statistically significant (Dunn test, $p<0.05$). σ_{PSII} showed an inverse trend than F_v/F_m with G01 having the highest absorption cross section (381.1 Å^2 quanta^{-1}) (Figure 12c). Again, there were significant differences between this station and the northern and southern regions at the mouth of the Gulf (Dunn test, $p<0.05$). In general, an inverse relationship was detected between both variables, with a decrease of F_v/F_m when σ_{PSII} increased (ANNEXE 4).
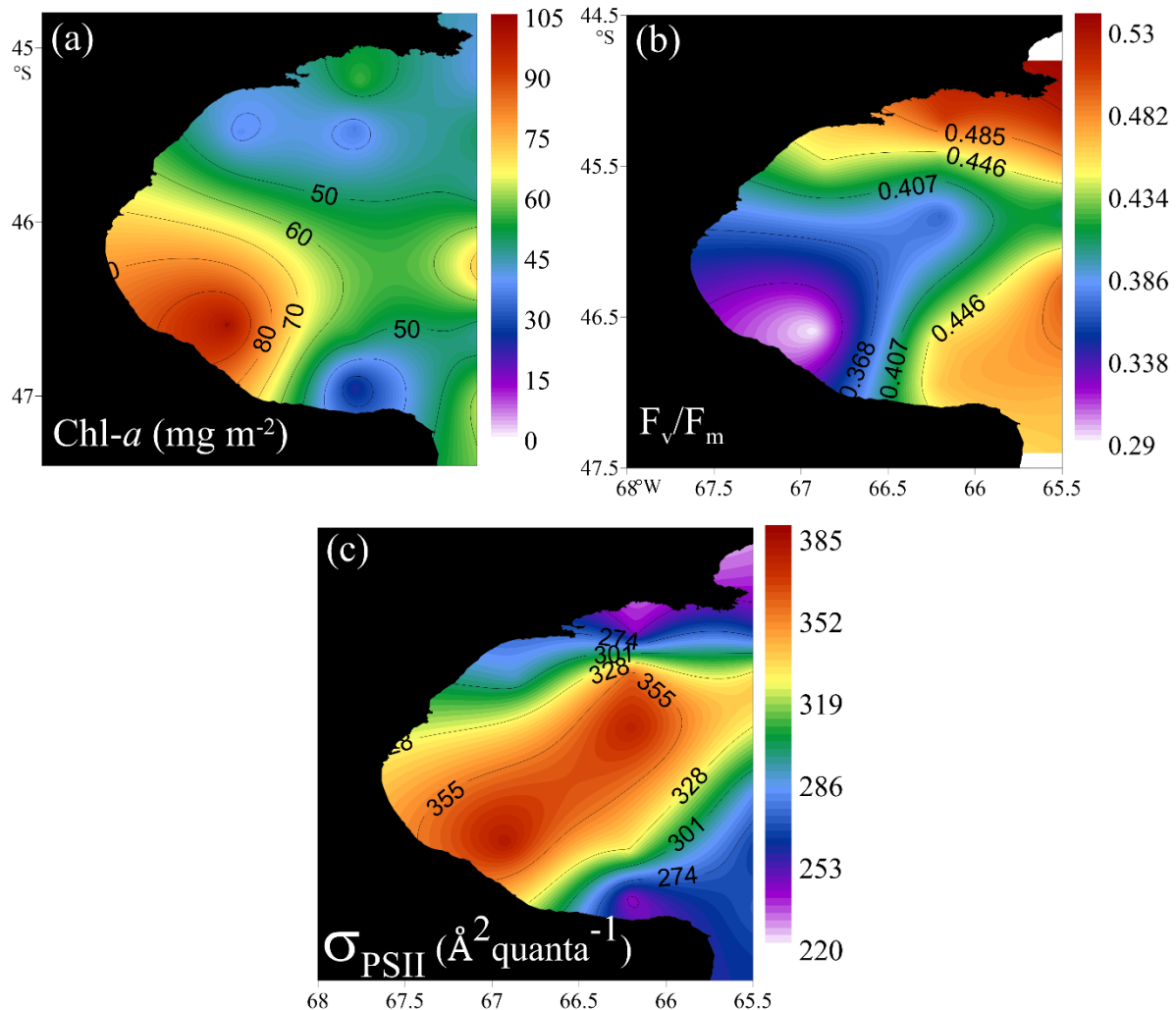
Figure 12: Horizontal distribution of a) Chl-*a* integrated in euphotic zone (pycnocline depth); b) maximum photochemical quantum yield (F_v/F_m) at Chl-*a* maximal depth; c) absorption cross section σ_{PSII} at Chl-*a* maximum depth.

1.5.10 Relation between the total particulate organic carbon and community organic carbon

Total particulate organic carbon (POC_T) at the depths of Chl-a maximum was highest at the G01 station (Table 2). The same pattern was detected for the particulate organic nitrogen (PON_T). Comparing the C:N ratio among stations, there was a clear difference between the coastal zone (values between 2-4) and the mouth of the gulf (>6 at G11-G16

stations), where values approached Redfield's ratio. Carbon contribution of the microbial community (POC_{MC}) to total POC_T was <29% in almost all the area, except at stations G13 and G14, in which it represented 53% and 38% respectively. In this area, and considering also the G01 station, the contribution of autotrophs (POC_A) to POC_T was higher than 20% and more important than that of heterotrophs. On the other hand, no major differences in the contribution of these large two groups were observed in the rest of the Gulf (see table 1, POC_A/ POC_T and POC_H/ POC_T ratios).

Table 2: Distribution of organic carbon and nitrogen in SJG. Abbreviations means: POCT: particulate organic carbon, PONT: particulate organic nitrogen, POCT/ PONT: Organic carbon and organic nitrogen ratio, POCMC: particulate organic carbon of microbial community, POCA: particulate organic carbon of autotrophs, POCH: particulate organic carbon of heterotrophs, POCMC/POCT: ratio between microbial community and total particulate organic carbon, POCA/ POCH: ratio between autotrophs and heterotroph particulate organic carbon, POCH/ POCT: ratio between heterotrophs and total particulate organic carbon.

Station	POC_T	PON_T	POC_T/ PON_T	POC_{MC}	POC_A	POC_H	POC_{MC}/ POC_T	POC_A/ POC_T	POC_H/ POC_T
G01	486.22	207.73	2.34	138.60	95.83	41.69	0.29	0.20	0.09
G04	142.17	20.72	6.86	22.04	7.58	14.22	0.16	0.05	0.10
G06	132.07	35.64	3.71	19.78	9.77	10.01	0.15	0.07	0.08
G07	209.87	94.89	2.21	52.95	29.02	20.39	0.25	0.14	0.10
G09	264.37	72.76	3.63	57.85	32.98	23.74	0.22	0.12	0.09
G10	366.29	99.58	3.68	34.38	10.14	24.19	0.09	0.03	0.07
G11	366.29	20.25	18.09	77.71	49.54	28.08	0.21	0.14	0.08
G13	274.06	47.23	5.80	144.02	114.46	29.20	0.53	0.42	0.11
G14	271.99	44.05	6.18	102.44	68.49	32.11	0.38	0.25	0.12
G15	290.86	55.07	5.28	54.37	17.25	25.73	0.19	0.06	0.09
G16	227.57	31.44	7.24	25.71	12.23	13.48	0.11	0.05	0.06

1.6   Discussion

1.6.1 Oceanographic features in the San Jorge Gulf

Based on salinity, two water masses we could identify in the present study, according to descriptions by Bianchi et al. (2005) and Painter et al. (2010). The inner Gulf was dominated by shelf waters (SW), with salinity > 33.4, and surface maxima of 33.7. This increase at the surface has already been previously identified (Krock et al 2016, Louge et al. 2004) and could be related to the excess of evaporation over precipitation in summertime (i.e. 3.5-6 cm month^{-1}; Lauge et. al. 2004). However, in the southeastern area this process is balanced by the entrance of low salinity coastal waters (LSCW), with salinity values between 33-33.4. LSCW, also referred to as the "Magellan plume" (Palma and Matano, 2012), take its origin from the Magellan Strait which are mixed with shelf waters and is also modified by the contribution of Patagonian rivers during their northward flow (Bianchi et al. 2005). LSCW arrive to the southern end of the Gulf, where the high energy dissipation of tides and the topography promote turbulent mixing (Tonini et al. 2006, Moreira et al., 2011). This could be corroborated with the very low Brunt–Väisälä Frequency values calculated for stations G11 to G13, which were indicative of the absence of stratification. Similarly, low Richardson numbers (high turbulence) characterized these stations. These conditions continued along the mouth of the Gulf, from stations G11 to G15 and were reflected in the homogeneity of the water column properties (see Figure 3). These results are in accordance with previous observations in the Gulf (Cucchi Colleoni and Carreto 2001, Krock et al. 2015, Papparazo et al. 2017). It is interesting to notice that the dissipation energy of tides in this area is one of the highest of the continental shelf, favoring the formation of a thermohaline front during summer and winter seasons (Acha et al 2004, Moreira et al. 2011, Glembocki et al. 2015). This is additionally important for its effect on vertical and horizontal advection of nutrients in the Gulf. Details of the dynamics and the effects of this front on the system behavior have been studied as part of the MARES project by Flores Melo (2017).

1.6.2   The role of turbulence in nutrient distribution at the SJG

The vertical distribution of nutrients was affected by water column structure, which was associated to isotherms configuration, marking a strong stratification at the central zone and a weakening or absence of stratification (as evidenced in the lack of a developed pycnocline and the low N values mentioned above) at both the coastal and the mouth areas of the Gulf. For the following discussion, we will focus on nitrate+nitrites dynamics, since these are the limiting nutrient in this zone (Akselman, 1996). The low-nutrient concentrations in the surface layer at the inner Gulf suggest oligotrophic conditions, particularly with regards to nitrogen. Nitrate limitation is evident in the low nitrate+nitrites: Silice and nitrate+nitrites: phosphates ratios compared with Redfield ratio in surface waters. Nitrate limitation has already been predicted for the study area according to seasonal cycles in temperate seas (Akselman, 1996) but only measured by Papparazo et al. (2017) with low resolution in the Gulf. Under these conditions, the turbulent or diffusive flux of nitrogen across the pycnocline helps mitigate N-limitation favoring phytoplankton growth (Lewis et al., 1986).

At the northern area, the pycnocline was deepened sinking the nutrient-depleted surface waters and therefore the nutricline. This can be explained by the circulation models proposed by Tonini et al. (2006), in which downwelling processes in northern zone were predicted as resulting from water circulation, while upwelling of deep waters due to westerly winds are expected in the southwest coast. The weak stratification at southwest station G01 could have resulted from the spread of this phenomenon, with surface waters being a mixture of both SW and LSCW, according to salinity values. Nonetheless, surface nitrate+nitrites remained low, but, high levels of Chl-*a* with high oxygen concentrations registered could indicate that this nutrient are being consumed by a photosynthetically active community.

Despite the relatively oligotrophic conditions in surface waters of the Gulf, it should be noted that the LSCW could fertilizing the southern region. Even if the concentration of nitrate+nitrites in LSCW waters was lower (6 µM) compared to bottom waters of the gulf (17 µM), it was comparable to shelf break concentrations for the same latitude (0-8 µM,

Painter et al., 2010, Valiadi et al., 2014). Its significance lies in that this nitrate+nitrites would be available for phytoplankton uptake in the upper layer. Moreover, satellite images show that the southern SJG is an area that is prone to eddies' formation and could move these waters to the center of the Gulf (Flores Melo, 2017). However, there is no conclusive information about nutrients in the LSCW, and the little information available is contradictory. A recent study performed in fall, when the vernal water column stratification is still present, showed a surface increase of nitrate+nitrites in the north and a decrease in the southern area of the SJG (Paparazzo et al., 2017), contrary to our results. Adding to that, Valiadi et al. (2014), indicate low levels of nitrate+nitrites associated with the LSCW. Conversely, Krock et al. (2015) reported high nitrate+nitrites levels in Beagle-Magellan Waters (BMW) associated with LSCW at the mouth of the Gulf. On the other hand, Carreto et al. (2007) hypothesize that nitrate+nitrites concentrations in the region are kept high by the influence of the west branch of the Malvinas current in the Gulf and the intense mixing of winds. However, our salinity values do not agree with the presence of these waters. Clearly, the BMW play an important role in sustaining the high levels of Chl-*a* recorded on the Patagonian coast (Romero et al., 2006). Apparently, there is also seasonal variability that modifies both, the volume of discharges from the Strait of Magellan (Piola and Rivas, 1997), as well as the income of Sub-Antarctic waters coming from Cape Horne (Song et al., 2016). These apparently contradictory results reflect the high hydrodynamism of the region. The intensive measures carried out in this work, together with the estimates of the dynamic stability of the water column, provide a valuable contribution to understanding the underlying processes that sustain the productivity of the gulf.

The formation of a seasonal nutricline is a characteristic feature in all temperate seas of the world (Childers et al., 2005, Coyle et al., 2008, Martin et al., 2010, Mojica et al., 2015). In the SJG, it was well developed in the central zone at 40-50m of depth, probably resulting from heavy nitrate+nitrites consumption by phytoplankton in the surface, and bacterial remineralization in deeper waters (Krock et al., 2015). However, this did not mean a limitation for the growth of phytoplankton, high levels of Chl-*a* recorded in this work, combined with the high biomass of zooplankton (Gimenez, 2017), show suitable conditions

for its growth. In concordance with this, Papparazo et al. (2017) estimate high primary production (expressed as nitrogen uptake) represented for both, new and regenerated production in equal percentages. It means that, one part of productivity in this area depends on nutrient supply from the mixing at the pycnocline.

In our work, dynamical stability (expressed by Ri) shown a significant negative exponential correlation with the nutrient gradient (Figure 7), which suggest that some degree of vertical flux of nutrients was possible across the pycnocline. Note that our data, based on stations separated in space and time, represent a snapshot of the physical-chemical conditions. Turbulence, on the other hand, is highly intermittent in time, limiting an accurate quantification of this process (Carr et al., 1995). However, the measurements at the fixed station, in which we attempted to overcome these limitations by means of a time series, showed the same correlation pattern. The destabilizing mechanisms are variable and related to weather (wind speed and storms) and physical processes such as the internal waves breaking. Furthermore, the tidal cycle could play a significant role in the input of new water to the Gulf. In our results, we could identify an upward progression of the pycnocline during the tidal rise (Fixed Station, Figure 6), which was probably transporting the nutrient-rich bottom waters 10m above their original position. Nevertheless, this situation was only observed during one cycle (SF1 to SF7) and not recurrently in the following cycles.

Several studies have calculated the flow of nutrients through the pycnocline, assuming turbulent conditions (Carr et al., 1995, Granata et al., 1995, Vidal et al., 1999, Agustí et al., 2001). However, when the conditions are adequate, diffusive transport of nutrients could be important (Hamilton et al., 1989, Oschlies et al., 2003, Dietze et al., 2004, Glessmer et al., 2008). In our work, LSCWs are likely to play an important destabilizing role as their input increased below the pycnocline during the tidal cycle (Figure 6). Yet, our estimate of convective flux was not significant, the estimated values of R_p were close to those needed for the formation of salt fingers. One possible explanation could be that this process actually happens when the hydrodynamic conditions are stable, particularly at low tide (Figure 6), but these salt fingers break quickly as the tide rises, where turbulent processes dominate. This

could explain the accumulation of Chl-*a* during low tide (Figure 6). The low resolution of our vertical measurement intervals limited the ability to effectively evaluate salt finger formation. Ideally, R_P calculations over 0.5m intervals would be more accurate to evaluate salt fingers formation (St. Laurent and Schmitt, 1998). Moreover, an intense and constrained sampling at the pycnocline, where changes in nutrient concentrations are greatest, is recommended to calculate nitrogen fluxes (Agusti et al. 2001). Despite this, our data are a good approach to highlight the underlying processes associated with the vertical nutrient input. In addition, Carr et al. (1995) recommended to use data from CTD moorings and nutrients for periods of 60 days for a good temporal resolution. Notwithstanding, the subsurface Chl-*a* maximum identified in this work and in previous studies (Cucchi Colleoni and Carreto, 2001) could be another evidence supporting the hypothesis of a potential nutrient replenishment across and around the pycnocline, favoring primary production (Lewis et al., 1986).

1.6.3 The significance of the maximum subsurface maximum Chl-*a* in summer.

The range of Chl-*a* values recorded agrees with previous studies in summer (Akselman, 1996, Cucchi Colleoni and Carreto 2001). In addition, the occurrence of two Chl-*a* hotspots in both the coastal zone (G01) and in the mouth of the gulf (G13), emerges as a characteristic feature that has already been documented in spring (Cucchi Colleoni and Carreto 2001). Although Chl-*a* concentrations may reach higher levels in spring (14 µg L^{-1}, Cucci Coleoni and Carreto, 2001), the Gulf remains one of the most productive places in summer compared to other gulfs in northern Patagonia (Solis, 1998, Williams et al., 2013). Similar Chl-*a* values in summer have been detected in the continental shelf and the shelf break by in-situ and satellite observations (Carreto et al., 2007, Valiadi et al., 2014, Glemboki et al. 2015, Gonçalves-Araujo et al, 2016). The occurrence of a coastal upwelling (Tonini et al., 2006) and a tidal front (Glemboki et al., 2015) can favor the accumulation of phytoplankton biomass. However, the subsurface Chl-*a* peaks are a characteristic feature at 20-50 m depth along the central and southern part of the gulf, associated with the thermocline and indirectly with the nutricline. Martin et al. (2010) showed that, for the Arctic Ocean and when

subsurface Chl-*a* maximum is present, the Chl-*a* inventories with satellite images could be underestimated by a factor of 3 to 5. The vertical phytoplankton distribution in the SJG suggests a similar situation, which highlights the need of further consideration to improve remote biomass estimations.

1.6.4 Microbial community composition and physiological state in relation to environmental conditions

Autotrophic picoplankton dominated the microbial community in terms of density and biomass, suggesting the importance of this group for summer primary production in the SJG. By contrast, nano- and micro-phytoplankton were observed as minor components of plankton communities, which contrast with higher densities recorded in previous studies (Akselman 1996, Krock et al., 2015).

The tb-RDA results suggest that temperature (or N), nutrient availability and dynamic stability are the main factors controlling the community. The fit of the model was good (52%), considering that usually ecological data are noisy so that it is unlikely to obtain high values of r^2 (Legendre and Legendre, 1998).

The pico-EUK was associated to low-temperature areas (weak stratification) with high nitrates+nitrites concentrations. Although these groups tend to predominate in stratified and low turbulent environments (Glibert, 2016), they grow at maximum rates using nitrates as the main resource. This would explain its distribution in areas where dynamic stability was low, allowing sporadic inputs of nutrients through the pycnocline. Conversely, pico-CYAN were associated with dynamically stable areas (Ri) with low nutrients levels and higher temperatures (high N), which could be explained by their use of ammonium as a nitrogen source (Glibert, 2016). The remineralization of the organic nutrients by H-BACT could be providing the necessary nutrients to the pico-CYAN (Legendre and Rassoulzadegan, 1995), which is inferred by the appearance of the overlapping biomass peaks of both groups.

From a functional-traits perspective, small cells require less nutrients to survive and are more efficient in nutrient uptake because of their large surface to volume ratio (Veldhuis et al., 2005, Litchman & Klausmeier, 2008, Finkel et al., 2010). However, variations in physiological traits rather than cell size alone, allow them to survive in a dynamically stable and nutrient-impoverished environment (Litchman and Klausmaier 2008, Mojica et al., 2015). The characteristics of the PSII photosystem are often used to evaluate the physiological stress of cells. However, PSII features vary among taxa and it could generate greater variability than that caused by the environment (Fishwik et al., 2006, Suggett et al., 2009). In our results, F_v/F_m and σ_{PSII} were inversely correlated. This is usual in natural populations related to the shift of microbial composition and the water column stability (Aiken et al., 2004, Fishwick et al., 2006, Moore et al., 2005, 2006). In areas dominated by pico-plankton F_v/F_m was low, accompanied by high values of σ_{PSII}. Our results agreed with measurements made in pico-CYAN or pico-EUK populations, with F_v/F_m ranging between 0.38-0.43and 0.29-0.38 respectively (Cermeño et al., 2005, Fishwik et al., 2006, Suggett et al., 2009). The reduced values of F_v/F_m on the west coast fall within this range and, added to the high values of oxygen saturation and the high concentration of Chl-*a*, its seems to be related more to an effect of the high density of pico-CYAN imposing its taxonomic signature than to nutrient stress of cells. Although within the Gulf the picoplankton had the highest values of σ_{PSII}, it was low compared to this group in other environments of the world (Cermeño et al., 2005, Moore et al., 2006), but it fell within the expected range for these groups (Suggett et al., 2009). For this reason and considering that the highest levels of oxygen saturation were associated with the presence of these groups, the community appeared to be in good physiological conditions, being photosynthetically active and able to accumulate biomass.

DIAT and DINO were related to low Ri and high nutrient availability. As might be expected, they accumulated in more turbulent areas, in the north and the southern end of the gulf in agreement with the results from Akselman (1996) during summer. Their physiological growth conditions were optimal, presenting the highest values of F_v/F_m and lowest of σ_{PSII}.

Although our analysis was carried out with a natural microbial community, where the taxonomic signature of each group is masked by the presence of others, our values coincided with those reported in the literature for microphytoplankton in culture (Suggett et al., 2009). This group usually has low sigma values associated with a reduction of the area of the photosynthetic antenna (reduce σ_{PSII}), to increase the efficiency in capturing photons in areas of high turbulence and low light (Suggett et al., 2009). Despite the apparent good physiological conditions, they did not reach high density. One explanation for this apparent paradox is the presence of an intense zooplankton grazing preventing phytoplankton accumulation. This hypothesis is supported by the presence of important spawning sites for commercial fish (Gongora et al., 2012) which may feed on phytoplankton in this area and the high zooplankton an microzooplankton (CIL) densities observed in the mouth and center of the Gulf (Gimenez, 2017).

POC is an estimator of living and dead plankton biomass (phytoplankton, bacteria, zooplankton, fecal pellets, continental detritus, etc.), which is an indicator of the productivity of the system. The mean POC concentration observed for the Gulf (275.61 mg m^{-3}) agrees with previous concentrations found in the southern Patagonian shelf in summer (300 mg m^{-3}; Gonçalves-Araujo et al., 2016). However, higher concentrations were measured throughout the southern coast of the Gulf (366-486 mg m^{-3}), with the maximum occurring at station G01, in coincidence with the high levels of Chl-*a* recorded in this sector. Nonetheless, as POC represent a mixture of plankton material, the POC:PON ratio (C:N) could be an useful tool to discriminate phytoplankton from heterotrophs and detritus. Phytoplankton generally presents a C:N ratio between 6 and 10, zooplankton and bacteria ranges between 3 to 6, and a C:N ratio >12 has being considered as detritus organic matter (Savoye et al., 2003 and references therein). In the Gulf, the ratio was generally < 6, which highlights the importance of the heterotrophic component. This supports our hypothesis of a high secondary production that would be the main consumers the phytoplankton (especially microphytoplankton) preventing its accumulation. This is particularly evident at station G01 where PON levels were the highest of the Gulf.

Throughout the mouth of the Gulf (G13 to G16) the C: N ratio was > 6, but the contribution of autotrophs was low (see table 2, POC_A / POC_T), except for G13 station where it reached 43%. This means that the increase in C: N ratio could be due to the degradation of the organic matter, given that PON is usually degraded faster than POC. High concentrations of free H-BACT were found on surface waters (data not shown) and decreased in depth, which could indicate two possibilities. One is that the degradation process started early on the surface of the euphotic layer and then continued below the pycnocline but not exclusively by free H-BACT. The other explanation is the formation of detrital aggregates known as "marine snow", where bacteria could attach to the particulate material, accelerating the degradation process (Alldredge et al., 1986). In this work the biomass of particle-attached bacteria was not analyzed, but this fraction could be very important considering that the heterotrophic carbon estimated in this study contributed only 12% of the total POC, supported by the decrease of oxygen in depth, possibly due to bacterial respiration. This demonstrates the limitation of the use of these ratios to predict the origin of the organic matter and highlights the importance of having information about the microbial community in order to understand the biogeochemical cycles in the water column. Both data combined represent a powerful tool to begin to inquire about the biological processes involved in the carbon cycle in the Patagonian coasts.

1.7 CONCLUSIONS

In this study we attempted to understand the functioning of the San Jorge Gulf's planktonic ecosystem and its productive capacity through the analysis of the microbial community (autotrophic and heterotrophic) and its relationship with the prevailing environmental conditions during the austral summer. The structuring of the microbial assemblages mostly depended on temperature (stratification) and inorganic nutrients availability. The importance of these parameters has been already documented for the Gulf (Akselman, 1996, Cucchi Colleoni and Carreto, 2001) and other sectors of the Argentine shelf (Araujo et al., 2016). However, in this work it was possible to detect for the first time in the Argentine coastal area how the turbulent processes linked to tides and the entry of

LSCW rich in nutrients favor the rupture of the pycnocline and modify the N-limiting conditions, allowing to know the explanatory mechanisms for the productivity of the community.

Nitrate+nitrites inputs are sporadic and appear to be rapidly consumed by autotrophic cells, preventing their accumulation in the euphotic zone. The good physiological state of these groups suggests that light and nutrient conditions were favorable for their growth. Particularly, the pico-EUK reached biomass peaks in the southern part of the Gulf, in association with high levels of Chl-*a* and high percentage of oxygen saturation. The pico-CYAN bacteria were also abundant and associated with the H-BACT, indicating a possible preference towards ammonium over nitrate, which allowed them to dominate in more stable and strongly stratified areas towards the north of the Gulf. Associated with these groups were the Dino-MIXO, which possibly feed on these small cells, supplying their phosphorus and nitrogen requirements.

On the other hand, microplankton were found preferentially in the northern Gulf area, but at low densities (DIAT, DINO and CIL). The high levels of POC recorded in the region explain the community's ability to generate organic matter. The C: N ratio shows that the community was heavily grazed. It is likely that there is selective grazing pressure, towards large cells, which is consistent with the content of fecal pellets observed by Masse-Beaulne (2017), where there was a high incidence of microphytoplankton. Bianchi et al. (2005) estimated the Gulf behaved as a source of CO_2 from the ocean to the atmosphere. Although our estimated autotrophic: heterotrophic ratio agrees with their results, it is possible that the Gulf maintains a high primary productivity in summer, which cannot be directly perceived since it does not accumulate as Chl-*a*, because of the high system turnover rate. This would indicate high secondary productivity and, possibly, high carbon export to deep waters. In this way, although CO_2 can escape into the atmosphere, the biological pump probably contributes significantly to CO_2 drawdown. In conclusion, and responding to our initial question, the San Jorge Gulf can be considered as a productive system during summer thanks to the prevailing physical processes that sustain nutrient inputs through the pycnocline.

CONCLUSION GÉNÉRALE

Cette étude visait à caractériser la variabilité spatiale dans la communauté microbienne dans le GSJ, en relation avec les facteurs biologiques et environnementaux qui la contrôlent pendant la saison estivale.

Le premier objectif de ce projet de recherche a été d'évaluer les caractéristiques dynamiques de la colonne d'eau et leurs impacts sur la dynamique des nutriments. Les caractéristiques océanographiques hétérogènes du golfe génèrent différentes conditions dynamiques, ce qui affecte de manière significative la disponibilité des nutriments dans la couche euphotique. En général, la colonne d'eau était stratifiée et appauvrie en éléments nutritifs à la couche de surface. Malgré les conditions oligotrophes apparentes, nous avons détecté le transfert de nutriments des eaux plus profondes vers la surface au niveau de la pycnocline en utilisant d'une approximation dynamique (nombre Richardson). Les observations effectuées durant la série temporelle à la station fixe suggèrent que ces processus pourraient être expliqués par l'effet combiné de la marée et du cisaillement des masses d'eau. En outre, dans la partie sud-est du golfe la présence d'un front de marée bien défini (Glemboki et al., 2015) a permis le renouvellement de nutriments dû au mélange vertical intense.

De plus, il a été possible d'analyser les processus de double diffusion associés à l'entrée des eaux à faible salinité de sub-surface, originaire du détroit de Magellan. Les faibles valeurs de Rp indiquent la possibilité de formation de doigts de sel mais nos instruments n'ont pas eu la résolution suffisante pour obtenir des résultats significatifs. D'après les données obtenues dans la station fixe, il est probable que les eaux à faible salinité favorisent la formation de doigts de sel lorsque les conditions hydrodynamiques sont stables, à marée basse, mais ces doigts de sel se brisent rapidement à fur et mesure que la marée monte, où les processus

turbulents dominent. Ces résultats rejettent notre hypothèse, démontrant que dans des zones stratifiées, des événements de mélange turbulents sporadiques se produisent et sont importants pour le maintien d'un de Chl-*a* maximale en sous-surface.

Le deuxième objectif était de décrire les modes de distribution de la communauté microbienne en fonction des variables environnementales. En accord avec notre hypothèse initiale, la disponibilité des nutriments module la composition et l'abondance de la communauté microbienne. Cependant, la structuration des assemblages dépend fortement de la stratification, dans la colonne d'eau, notamment contrôlée par la température. Ces paramètres ont déjà été documentés comme importants dans d'autres secteurs de la plate-forme argentine et d'autres mers tempérées du monde (Gonçalves-Araujo et al., 2016, Mojica et al., 2016). Dans cette étude, c'est le phytoplancton à petite taille, le pico-plancton, qui dominait dans le golfe. Cependant, les caractéristiques des environnementales ont affecté différemment chaque sous-groupe. Le pico-phytoplancton eucaryote dominait principalement dans la zone sud-est, laquelle présentait des concentrations en nutriments élevées, ainsi qu'une faible stratification dans la colonne d'eau, tandis que dans la zone sud-ouest, les pico-eucaryote et les pico-cyanobactéries était les groupes dominants. Dans la zone centrale (composé par le centre et l 'embouchure du golfe), un assemblage de pico-cyanobactéries bactéries hétérotrophes était dominant, dans des eaux plus stratifiées et appauvries en nutriments. D'autre part, le microplancton était présent préférentiellement dans la zone nord du golfe, mais à faibles densités.

En ce qui concerne le troisième objectif, l'état physiologique du phytoplancton est optimal pour le développement du chaque sous-groupe phytoplancton en la saison estivale, ce qui suggère que les conditions de lumière et de nutriments sont favorables à leur croissance. Nos résultats montrent que les variations détectées sont plus associées à un effet de la composition taxonomique qu'à un stress physiologique, comparant nos données à celles obtenues dans d'autres groupes phytoplanctoniques du monde (Table 3). Étant donné que les conditions environnementales étaient favorables à la croissance du phytoplancton et à la faible accumulation de biomasse des microorganismes autotrophes, il est possible que la

communauté ait été contrôlée par la prédation. Le rapport C: N montre que la communauté se trouve fortement soumise à la prédation par broutage. En particulier, nous avons fait l'hypothèse qu'il y ait une pression de broutage sélective sur les grosses cellules, ce qui est cohérent avec les données de pelotes fécales obtenues par Masse-Beaulne (2017), où il y avait une forte présence de micro-phytoplancton. Ces résultats contrastent avec ceux obtenus par Bianchi et al. (2005), qui considère le golfe comme une source de CO_2. Bien que l'équilibre entre autotrophes et hétérotrophes soit en accord avec ces affirmations, il est possible que le golfe maintienne une productivité primaire élevée en été, mais cela ne peut pas être perçu directement en raison du taux de renouvellement élevé du phytoplancton. Cela se traduit par une productivité secondaire élevée et par une possible exportation de carbone vers les eaux profondes. De cette façon, bien que le CO_2 puisse s'échapper dans l'atmosphère, le pompage biologique peut entraîner le fonctionnement global du système comme puits de CO_2. D'ailleurs, les taux élevés de production primaire enregistrés en automne contribuent au soutien de cette hypothèse (Papparazo et al., 2017).

Table 3 : L'efficacité quantique maximale de la photochimique du PSII (F_v / F_m) dans différentes zones du monde et cette étude.

Groupe d'algues	F_v/F_m	Site d'étude	Auteurs
Communauté phytoplanctonique naturelle			*Cette étude*
Dominé par Pico-eucaryotes	0.29-0.38		
Dominé Cyanobactéries	0.38-0.43		
Dominé micro-plancton (Diatomées et dinoflagellés)	0.44-0.54		
Communauté phytoplanctonique naturelle		Écosystème de Benguela	*Fishwik et al. 2006*
Dominés par Flagellés	0.25-0.46		
Diatomées	0.4-0.57		
Dinoflagellés	0.52-0.57		
Classes isolées des communautés naturelles de phytoplancton		Ría de Vigo, Espagne	*Cermeño et al. 200!*
< 5 µm	0.49±0.04		
5-20 µm	0.42±0.04		
>20 µm	0.53±0.01		
Monocultures			*Suggett et al. 2009*
Pico-eucaryotes	0.3-0.4		
Cyanobactéries	0.1-0.4		
Cyanobactéries fixatrices d'azote	0.6-0.65		
Diatomées	0.5-0.64		
Dinoflagellés	0.42-0.55		

PERSPECTIVES FUTURES DE RECHERCHE

Le présent travail a tenté d'aborder l'écologie des communautés microbiennes d'un point de vue multidisciplinaire, en portant attention aux processus physiques qui peuvent agir dans la colonne d'eau favorisant la disponibilité des nutriments dans la couche euphotique, et donc à maintenir une production primaire élevée. Cependant, il reste encore plusieurs questions à répondre qui pourrait permettre de compléter l'information obtenue, afin de mieux comprendre l'écosystème du golfe de San Jorge.

Un aspect intéressant à prendre considération est l'estimation des flux d'éléments nutritifs provenant des eaux profondes. Dans cette étude, il n'a pas été possible de se procurer des mesures détaillées pour estimer des flux d'azote dans la couche euphotique. La compréhension des mécanismes contrôlant la production primaire locale et la croissance de la biomasse du phytoplancton nécessites davantage de recherche. Les seules mesures de production primaire ont été réalisées en termes d'azote à l'automne (Papparazo et al., 2017), mais avec un faible niveau de résolution spatial et temporelle.

Nos résultats ont montré que les pic-eucaryotes étaient dominants dans la partie sud du Golfe et en étroite relation avec des niveaux élevés d'oxygène et Chl-*a*. L'importance de ces groupes dans la production nouvelle ainsi que leurs rôles dans les réseaux trophiques pélagiques a déjà été documenté dans des autres milieux marins du monde (Worden 2006). Pour cette raison, il serait important de faire des estimations de la production de carbone en tenant compte de la gamme de tailles pour évaluer la contribution en termes du carbone des différents groupes.

En plus de la production de carbone, un autre facteur à étudier est la formation et l'exportation d'agrégats el leur signification pour la reminéralisation de la matière organique. Une diminution marquée du POC en profondeur associée à une forte diminution de l'oxygène a été observée, ce qui est probablement lié à la respiration bactérienne. Dans nos observations des échantillons en laboratoire, nous avons pu remarquer la formation de ces agrégats caractérisés par une riche communauté microbienne hétérotopiques et autotrophiques. Nous savons qu'en présence des hautes quantités de bactéries, l'existence de ces agrégats accélère

le processus de décomposition. Par conséquent, leur étude est très importante afin de connaître la dynamique de la reminéralisation des nutriments et leur disponibilité pour les producteurs primaires.

À ce jour, ce travail présente les seules mesures effectuées concernant l'état physiologique du phytoplancton et de sa relation avec les différents groupes taxonomiques dans le GSJ. Cependant, il est nécessaire de prendre en considération que nos résultats incluent la communauté autotrophe complète, avec les inférences faites concernant l'état physiologique basé sur l'information recueillie de la littérature avec d'autres espèces dans d'autres parties du monde. Pour mieux comprendre et associer les paramètres environnementaux, les mesures F_v/F_m et σ_{PSII} devraient être effectuées de façon saisonnière dans le GSJ afin d'évaluer leur signification écologique de façon plus approfondie.

Enfin, le GSJ semble avoir une productivité secondaire élevée en été, exprimée par les faibles niveaux de C: N et la prolifération d'une énorme quantité de larves d'espèces de grand intérêt commercial comme la crevette (*Pleoticus muelleri*), le merlu (*Merluccius hubbsi*) et le crabe royal (*Lithodes santolla*). Cependant, non seulement le micro / mésozooplancton contribuent au pool de carbone, mais le contrôle top-down de la lyse virale est également un facteur nécessaire qui n'a pas été considéré dans ce travail. La présence de virus est généralement corrélée avec des bactéries et du pico-plancton qui servent d'hôtes (De Corte et al 2016, Mojica et al 2015b, Yang et al., 2010). Les virus sont capables d'éliminer entre 20 et 40% de la biomasse microbienne par jour, ce qui affecte la succession et donc la structure des communautés microbiennes et le bilan de carbone de l'écosystème (Suttle, 2007). Commencer à les considérer au sein de la communauté microbienne devra être un objectif majeur dans la future afin de mieux interpréter les cycles biogéochimiques dans les écosystèmes côtiers.

RÉFÉRENCES BIBLIOGRAPHIQUES

Acha, E. M., Mianzan, H. W., Guerrero, R. A., Favero, M., & Bava, J., 2004. Marine fronts at the continental shelves of austral South America: Physical and ecological processes. *Journal of Marine Systems*, 44(1-2), 83-105 http://doi.org/10.1016/j.jmar sys.2003.09.005.

Agustí, S., Duarte, C. M., Vaque, D., Hein, M., Gasol, J. M., and Vidal, M., 2001. Food-web structure and elemental (C, N and P) fluxes in the eastern tropical North Atlantic. *Deep Sea Research Part II*, 48(10), 2295-2321. http://doi.org/10.1016/S09 67-0645(00)00179-X.

Aiken, J., Fishwick, J., Moore, G., ANPemberton, K., 2004. The annual cycle of phytoplankton photosynthetic quantum efficiency, pigment composition and optical properties in the western English Channel. *Journal of the Marine Biological Association of the United Kingdom*, 84(2), 301-313. http://doi.org/10.10 17/S0025315404009191h

Akselman, R., 1996. Estudios ecológicos en el Golfo San Jorge y aguas adyacentes (Atlántico Sudoccidental). Distribución, abundancia y variación estacional del fitoplancton en relación a factores físico-químicos y la dinámica hidrológica. PhD Thesis, Universidad de Buenos Aires, Buenos Aires, Argentina, 244 pp.

Alldredge, A. L., Cole, J. J., and Caron, D. A., 1986. Production of heterotrophic bacteria inhabiting macroscopic organic aggregates (marine snow) from surface waters. *Limnology and Oceanography,* 31(1), 68-78.

Aminot, A., & Chaussepied, M., 1983. Manuel des analyses chimiques en milieu marin (No. 551.464 AMI). 395 pp.

Azam, F., Fenchel, T., Field, J. G., Gray, J. S., Meyer-Reil, L. A., and Thingstad, F., 1983. The Ecological Role of Water-Column Microbes in the Sea. *Marine Ecology Progress Series*, 10:257–263, https://doi.org/10.3354/meps010257.

Behrenfeld, M. J., and Falkowski, P. G., 1997. Photosynthetic rates derived from satellite-based chlorophyll concentration. *Limnology and Oceanography*, 42(1), 1-20. http://doi.org/10.4319/lo.1997.42.1.0001.

Belzile, C., Brugel, S., Nozais, C., Gratton, Y., and Demers, S., 2008. Variations of the abundance and nucleic acid content of heterotrophic bacteria in Beaufort Shelf waters

during winter and spring. *Journal of Marine Systems*, 74(3-4), 946-956. http://doi.org/10.1016/j.jmarsys.2007.12.010.

Belzile, C. and Gosselin, M., 2015. Free-living stage of the unicellular algae *Coccomyxa* sp. parasite of the blue mussel (Mytilus edulis): Low-light adaptation, capacity for growth at a very wide salinity range and tolerance to low pH. *Journal of Invertebrate Pathology*, 132, 201-207. http://doi.org/10.1016/j.jip.2015.10.006.

Bianchi, A. A., Bianucci, L., Piola, A. R., Pino, D. R., Schloss, I., Poisson, A. and Balestrini, C. F., 2005. Vertical stratification and air-sea CO_2 fluxes in the Patagonian shelf. Journal of Geophysical Research, 110(7), 1-10. http://doi.org/10.1029/2004JC00248 8.

Bisbal, G. A., 1995. The Southeast South American shelf large marine ecosystem. Evolution and components. *Marine Policy*, 19(1), 21-38. http://doi.org/10.1016/0308-597X(95)92570-W.

Blanchet, F. G., Legendre, P., Bergeron, J. A., and He, F., 2014. Consensus RDA across dissimilarity coefficients for canonical\nordination of community composition data. *Ecological monographs*, 84(3), 491-511. http://doi.org/10.1890/13-0648.1.

Carr, M. E., Lewis, M. R., Kelley, D., and Jones, B., 1995. A physical estimate of new production in the equatorial Pacific along 150°W. *Limnology and Oceanography.* http://doi.org/10.4319/lo.1995.40.1.0138.

Carreto, J. I., M. O. Carignan, N. G. Montoya, and A. D. Cucchi Colleoni, 2007. Ecología Del Fitoplancton en los sistemas frontales del Mar Argentino. *El Mar Argentino Y Sus Recursos Pesqueros*, 31(2016):11–31.

Cermeño, P., Estévez-Blanco, P., Marañón, E., and Fernández, E., 2005. Maximum photosynthetic efficiency of size-fractionated phytoplankton assessed by 14C uptake and fast repetition rate fluorometry. *Limnology and Oceanography*, 50(5), 1438-1446. http://doi.org/10.4319/lo.2005.50.5.1438.

Childers, A. R., Whitledge, T. E., and Stockwell, D. A., 2005. Seasonal and interannual variability in the distribution of nutrients and chlorophyll a across the Gulf of Alaska shelf: 1998-2000. *Deep-Sea Research Part II*, 52(1-2 SPEC. ISS.), 193-216. http://doi.org/10.1016/j.dsr2.2004.09.018.

Commendatore, M. G., Esteves, J. L., 2007. An assessment of oil pollution in the coastal zone of Patagonia, Argentina. *Environmental Management*, 40(5), 814-821. http://doi.org/10.1007/s00267-005-0221-3

Coyle, K. O., Pinchuk, A. I., Eisner, L. B., and Napp, J. M., 2008. Zooplankton species composition, abundance and biomass on the eastern Bering Sea shelf during summer: The potential role of water-column stability and nutrients in structuring the zooplankton community. *Deep-Sea Research Part II*, 55(16-17), 1775-1791. http://doi.org/10.1016/j.dsr2.2008.04.029.

Cucchi Colleoni, D.Carreto, J. I., 2001. Variacion estacional de la biomasa fitoplanctonica en Golfo San Jorge. *El Mar Argentino y sus recursos pesqueros*, 31:11–31.

Cullen, J. J., Franks, P. J. S., Karl, D. M., and Longhurst, A., 2002. Physical influences on Marine Ecosystem dynamics. *The sea,* 2002 (12), p. 297-336.

Dietze, H., Oschlies, A., & Kähler, P., 2004. Internal-wave-induced and double-diffusive nutrient fluxes to the nutrient-consuming surface layer in the oligotrophic subtropical North Atlantic. *Ocean Dynamics,* 54(1), 1-7. http://doi.org/10.1007/s10236-003-0060-9.

Falkowski, P. G., 1994. The role of phytoplankton photosynthesis in global biogeochemical cycles. *Photosynthesis Research*, 39(3), 235-258. http://doi.org/10.1007/BF00014586.

Falkowski, P. G., Katz, M. E., Knoll, A. H., Quigg, A., Raven, J. A., Schofield, O., and Taylor, F. J. R., 2004. The evolution of modern eukaryotic phytoplankton. *Science*, 305(5682), 354-360. http://doi.org/10.1126/science.1095964.

Falkowski, P., and Kolber, Z., 1995. Variations in Chlorophyll Fluorescence Yields in Phytoplankton in the World Oceans. *Australian Journal of Plant Physiology*, 22(2), 341. http://doi.org/10.1071/PP9950341.

Fernandez, M., Carreto, J. I., Mora, J., and Roux, A., 2005. Physico-chemical characterization of the benthic environment of the Golfo San Jorge. *Journal of the Marine Biological Association of the United Kingdom*, 6(85), 1317-1328. http://doi.org/10.1017/S002531540501249X.

Fernández, M., Mora, J., Roux, A., Cucchi Colleoni, D. A., and Gasparoni, J. C., 2008. New contribution on spatial and seasonal variability of environmental conditions of the Golfo San Jorge benthic system, Argentina. *Journal of the Marine Biological Association of the United Kingdom*, 88(2), 227-236. http://doi.org/10.1017/S0025315408000465.

Finkel, Z. V., Beardall, J., Flynn, K. J., Quigg, A., Rees, T. A. V, and Raven, J. A., 2010. Phytoplankton in a changing world: Cell size and elemental stoichiometry. *Journal of Plankton Research*, 32(1), 119-137. http://doi.org/10.1093/plankt/fbp098.

Fishwick, J. R., Aiken, J., Barlow, R., Sessions, H., Bernard, S., and Ras, J., 2006. Functional relationships and bio-optical properties derived from phytoplankton pigments, optical and photosynthetic parameters; a case study of the Benguela ecosystem. *Journal of the Marine Biological Association of the United Kingdom*, 86(6), 1267-1280. http://doi.org/10.1017/S0025315406014287.

Flores Melo, E. X., 2017. Réponse du phytoplancton au cycle de marée vive-eau/morte-eau, dans en front de marée au sud du golfe San Jorge, Patagonie argentine. Master's thesis, University of Quebec in Rimouski, Quebec.

Fujiki, T., Matsumoto, K., Mino, Y., Sasaoka, K., Wakita, M., Kawakami, H., Saino, T., 2014. Seasonal cycle of phytoplankton community structure and photophysiological state in the western subarctic gyre of the North Pacific. *Limnology and Oceanography*, 59(3), 887-900. http://doi.org/10.4319/lo.2014.59.3.0887.

Galperin, B., Sukoriansky, S., and Anderson, P. S., 2007. On the critical Richardson number in stably stratified turbulence. *Atmospheric Science Letters*, 8(3), 65-69. http://doi.org/10.1002/asl.153.

Garcia, H. E., & Gordon, L. I., 1992. Oxygen solubility in seawater: Better fitting equations. *Limnology and Oceanography*, 37(6), 1307-1312. http://doi.org/10.4319/lo.1992.37.6.1307.

Gill, A. E., 1982. Atmosphere-ocean Dynamics. International Geophysics. Elsevier.

Gimenez, E., 2017. Composition, distribution spatiale et structure trophique de la communauté zooplanctonique dans le Golfe San Jorge en Patagonie Argentine. Master's thesis, University of Quebec in Rimouski, Quebec.

Glembocki, N. G., Williams, G. N., Góngora, M. E., Gagliardini, D. A., and Orensanz, J. M. (Lobo), 2015. Synoptic oceanography of San Jorge Gulf (Argentina): A template for Patagonian red shrimp (*Pleoticus muelleri*) spatial dynamics. *Journal of Sea Research*, 95, 22-35. http://doi.org/10.1016/j.seares.2014.10.011.

Glessmer, M. S., Oschlies, A., and Yool, A., 2008. Simulated impact of double-diffusive mixing on physical and biogeochemical upper ocean properties. *Journal of Geophysical Research: Oceans* 113(C8)., 113.

Glibert, P. M., 2016. Margalef revisited: A new phytoplankton mandala incorporating twelve dimensions, including nutritional physiology. *Harmful Algae,* 55, 25-30. http://doi.org/10.1016/j.hal.2016.01.008.

Gómez, F., Moreira, D., and López-García, P., 2011. Filogenia molecular de dinoflagelados Avances en el estudio de los dinoflagelados (Dinophyceae) con la filogenia molecular. *Hidrobiológica*, 21(213), 343-364.

Gonçalves-Araujo, R., de Souza, M. S., Mendes, C. R. B., Tavano, V. M., and Garcia, C. A. E., 2016. Seasonal change of phytoplankton (spring vs. summer) in the southern Patagonian shelf. *Continental Shelf Research*, 124, 142-152. http://doi.org/10.1016/j.csr.2016.03.023.

Gongora, M. E., Gonzalez Zevallos, D., Pettovello, A., and Mendia, L., 2012. Caracterización de las principales pesquerias del golfo San Jorge Patagonia, Argentina. *Latin American Journal of Aquatic Research,* 40(1), 1-11. http://doi.org/10.3856/vol40-issue1-fulltext-1.

Granata, T., Wiggert, J., and Dickey, T., 1995. Trapped, near-inertial waves and enhanced chlorophyll distributions. *Journal of Geophysical Research*, 100, 20793-20804.

Greene, R., Geider, R., Kolber, Z., and Falkowski, P. G., 1992. Iron induced changes in light harvesting and photochemical energy conversion processes in eukaryotic marine-algae. *Plant Physiology*, 100, 565-575.

Gregg, W. W., Casey, N. W., and McClain, C. R., 2005. Recent trends in global ocean chlorophyll. *Geophysical Research Letters*, 32(3), 1-5. http://doi.org/10.1029/2004 GL021808.

Hamilton, J. M., Lewis, M. R., and Ruddick, B. R., 1989. Vertical fluxes of nitrate associated with salt fingers in the world's oceans. *Journal of Geophysical Research: Oceans*, C2(2), 2137-2145.

Hans van Hare, L. M., Zimmerman, S, J. T. F., Ridderinkhoaf, H., and Malschaert, H., 1999. Strong inertial currents and marginal internal wave stability in the central North Sea. *Geophysical Research Letters*, 26(19), 2993-2996.

Hillebrand, H., Dürselen, C.-D., Kirschtel, D., Pollingher, U., and Zohary, T., 1999. Biovolume Calculation for Pelagic and Benthic Microalgae. *Journal of Phycology*, 35(2), 403-424. http://doi.org/10.1046/j.1529-8817.1999.3520403.x.

Jackett, D. R., & Mcdougall, T. J., 1995. Minimal Adjustment of Hydrographic Profiles to Achieve Static Stability. *Journal of Atmospheric and Oceanic Technology.* http://doi .org/10.1175/1520-0426(1995)012<0381:MAOHPT>2.0.CO;2.

Kolber, Z., Prasil, O., and Falkowski, P. G., 1998. Measurements of variable fluorescence using fast repetition rate techniques: defining methodolgy and experimental protocols. *Biochimica et Biophysica Acta (BBA)-Bioenergetics*, 1367, 88-106.

Krock, B., Borel, C. M., Barrera, F., Tillmann, U., Fabro, E., Almandoz, G. O., Lara, R. 2015. Analysis of the hydrographic conditions and cyst beds in the San Jorge Gulf, Argentina, that favor dinoflagellate population development including toxigenic species and their toxins. *Journal of Marine Systems*, 148, 86-100. http://doi.org/10.1016/j.jmarsys.2015.01.006.

Legendre, L., and Rassoulzadegan, F., 1995. Plankton and nutrient dynamics in marine waters. *Ophelia*, 41(1), 153-172. http://doi.org/10.1080/00785236.1995.10422042.

Legendre, P., and Gallagher, E. D., 2001. Ecologically meaningful transformations for ordination of species data. *Oecologia*, 129(2), 271-280. http://doi.org/10.1007/s0044 20100716.

Legendre, P., and L. Legendre, 1998. Numerical Ecology: Second English Edition. Developments in environmental modelling 20., Montréal, Canada, 322 pp.

Lewis, M. R., Hebert, D., Harrison, W. G., Platt, T., and Oakey, N. S., 1986. Vertical nitrate fluxes in the oligotrophic ocean. *Science (*New York, N.Y.), 234(4778), 870-873. http://doi.org/10.1126/science.234.4778.870.

Litchman, E., and Klausmeier, C. A., 2008. Trait-Based Community Ecology of Phytoplankton. *Annual Review of Ecology, Evolution, and Systematics*, 39(1), 615-639. http://doi.org/10.1146/annurev.ecolsys.39.110707.173549.

Louge, E. B., Reta, R., Santos, B. A., and Hernandez, D. R., 2004. Variaciones interanuales (1995-2000) de la temperatura y la salinidad registradas en los meses de enero en el Golfo San Jorge y aguas adyacentes (43 S-47 S). *Revista de Investigacion y Desarrollo Pesquero*, 16, 27-42.

Mann, K.H., and J.R. Lazier, 2006. Dynamics of Marine Ecosystems: Biological-Physical Interactions in the Oceans. *Blakwell Publishing*, USA, 496 pp.

Margalef, R., 1978. Life-forms of phytoplankton as survival alternatives in an unstable environment. *Oceanologica acta*, 1, 493–509.

Martin, J., J. É. Tremblay, J. Gagnon, G. Tremblay, A. Lapoussière, C. Jose, M. Poulin, M. Gosselin, Y. Gratton, and C. Michel., 2010. Prevalence, structure and properties of subsurface chlorophyll maxima in Canadian Arctic waters. *Marine Ecology Progress Series*, 412:69–84, https://doi.org/10.3354/meps08666.

Martin, P., L. Serio, A. Pescio, and W. Dragani, 2016. Persistencia de vientos superficiales del cuadrante este en estaciones costeras de la Patagonia. *Asociación Argentina de Geofísicos y Geodestas*, 40(2):87–97.

Massé-Beaulne, V., 2017. Métabolisme de la communauté microbienne et flux de carbone à court terme dans le golfe San Jorge, Patagonie (Argentine). Master's thesis, University of Quebec in Rimouski, Quebec, Canada, 121 p.

Matano, R. P., Palma, E. D., and Piola, A. R., 2010. The influence of the Brazil and Malvinas Currents on the Southwestern Atlantic Shelf circulation. *Ocean Science*, 6(4), 983-995. http://doi.org/10.5194/os-6-983-2010.

Maxwell, K., & Johnson, G. N., 2000. Chlorophyll fluorescence a practical guide. *Journal of Experimental Botany*, 51(345), 659-668. http://doi.org/10.1093/jxb/51.345.659.

McDougall, T. J., and Barker, P. M., 2011. Getting started with TEOS-10 and the Gibbs Seawater (GSW). *Oceanographic toolbox*, SCOR/IAPSO, 1-28.

Menden-Deuer, S., and Lessard, E. J., 2000. Carbon to volume relationships for dinoflagellates, diatoms, and other protist plankton. *Limnology and Oceanography*, 45(3), 569-579. http://doi.org/10.4319/lo.2000.45.3.0569.

Mino, Y., Matsumura, S., Lirdwitayaprasit, T., Fujiki, T., Yanagi, T., and Saino, T., 2014. Variations in phytoplankton photo-physiology and productivity in a dynamic eutrophic ecosystem: A fast repetition rate fluorometer-based study. *Journal of Plankton Research*, 36(2), 398-411. http://doi.org/10.1093/plankt/fbt118.

Mojica, K. D. A., van de Poll, W. H., Kehoe, M., Huisman, J., Timmermans, K. R., Buma, A. G. J. and Brussaard, C. P. D., 2015. Phytoplankton community structure in relation to vertical stratification along a north-south gradient in the Northeast Atlantic Ocean. *Limnology and Oceanography*, 60(5), 1498-1521. http://doi.org/10.1002/lno.10113.

Moore, C. M., Lucas, M. I., Sanders, R., and Davidson, R., 2005. Basin-scale variability of phytoplankton bio-optical characteristics in relation to bloom state and community structure in the Northeast Atlantic. *Deep- Sea Research Part I: Oceanographic Rese arch Papers*, 52(3), 401-419. http://doi.org/10.1016/j.dsr.2004.09.003.

Moore, C. M., Suggett, D. J., Hickman, A. E., Kim, Y.-N., Tweddle, J. F., Sharples and J. Holligan, P. M., 2006. Phytoplankton photoacclimation and photoadaptation in response to environmental gradients in a shelf sea. *Limnology and Oceanography*, 51(2), 936-949. http://doi.org/10.4319/lo.2006.51.2.0936.

Numerosky, N., 2004. Petróleo-gas-petroquímica: Facilidades portuarias 2. *Petrotecnia*, 45(2), 40-42.

Oksanen, J., F. G. Blanchet, M. Friendly, R. Kindt, P. Legendre, D. Mcglinn, P. R. Minchin, R. B. O'hara, G. L. Simpson, P. Solymos, M. Henry, H. Stevens, E. Szoecs, and H. Wagner. 2017. *Vegan: Community Ecology Package*. Vienna, https://CRAN.R-project.org/package=vegan.

Oschlies, A., Dietze, H., and Kähler, P., 2003. Salt-finger driven enhancement of upper ocean nutrient supply. *Geophysical research letters*, 30(23).

Painter, S. C., Poulton, A. J., Allen, J. T., Pidcock, R., and Balch, W. M., 2010. The COPAS'08 expedition to the Patagonian Shelf: Physical and environmental conditions during the 2008 coccolithophore bloom. *Continental Shelf Research*, 30(18), 1907-1923. http://doi.org/10.1016/j.csr.2010.08.013.

Palma, E. D., and Matano, R. P., 2012. A numerical study of the Magellan Plume. *Journal of Geophysical Research. Oceans,* 117(5), 01-16. http://doi.org/10.1029/2011JC007 750.

Palma, E. D., Matano, R. P., and Piola, A. R. (2008). A numerical study of the Southwestern Atlantic Shelf circulation: Stratified ocean response to local and offshore forcing. *Journal of Geophysical Research: Oceans*, 113(11), 1-22. http://doi.org/10.1029/20 07JC004720.

Paparazzo, F. E., Williams, G. N., Pisoni, J. P., Solís, M., Esteves, J. L., and Varela, D. E., 2017. Linking phytoplankton nitrogen uptake, macronutrients and chlorophyll-a in SW Atlantic waters: The case of the Gulf of San Jorge, Argentina. *Journal of Marine Systems*, 172(March), 43-50. http://doi.org/10.1016/j.jmarsys.2017.02.007.

Parkhill, J., Maillet, G., and Cullen, J. J. (2001). Fluorescence based maximal quantum yield for PSII as a diagnostic of nutrient stress. *Journal of Phycology*, 37(4), 517-529. http://doi.org/10.1046/j.1529-8817.2001.037004517.x.

Petrotecnia, 2004. Las terminales de hidrocarburos. Petrotecnia, 45(2), 26-37.

Piola, A. R., and A. Rivas. 1997. Corrientes en la plataforma continental. *El Mar Argentino Y Sus Recursos Pesqueros*, 1:119–132.

Putt, M. and Stoecker, D. K., 1989. An experimentally determined carbon: volume ratio for marine Foligotrichous ciliates from estuarine and coastal waters. *Limnology and Oceanography*, 34, 1097-1103.

Romero, S. I., Piola, A. R., Charo, M., & Eiras Garcia, C. A., 2006. Chlorophyll-a variability off Patagonia based on SeaWiFS data. *Journal of Geophysical Research: Oceans*, 111(5), 1-11. http://doi.org/10.1029/2005JC003244.

Savoye, N., Aminot, A., Tréguer, P., Fontugne, M., Naulet, N., and Kérouel, R. (2003). Dynamics of particulate organic matter $\delta 15N$ and $\delta 13C$ during spring phytoplankton blooms in a macrotidal ecosystem (Bay of Seine, France). *Marine Ecology Progress Series,* 255, 27-41. http://doi.org/10.3354/meps255027.

Schloss, I. R., Ferreyra, G. A., Ferrario, M. E., Almandoz, G. O., Codina, R., Bianchi, A. A. and Poisson, A., 2007. Role of plankton communities in sea-air variations in $pCO2$ in the SW Atlantic Ocean. *Marine Ecology Progress Series*, 332, 93-106. http://doi.org/10.3354/meps332093.

Schmitt, R. W., 2003. Observational and laboratory insights into salt finger convection. *Progress in Oceanography*, 56(3-4), 419-433. http://doi.org/10.1016/S0079-6611(03)00033-8.

Smyth, T. J., Pemberton, K. L., Aiken, J. and Geider, R. J., 2004. A methodology to determine primary production and phytoplankton photosynthetic parameters from Fast Repetition Rate Fluorometry. *Journal of Plankton Research*, 26(11), 1337-1350. http://doi.org/10.1093/plankt/fbh124.

Solis, M. 1998. Monitoring in Nuevo Gulf (Argentina): Analysis of Oceanographic Data by Geographic Information Systems (GIS). MSc. Thesis, International Institute for Infraestructural, Hydraulic and Environmental Engineering (IHE), Delft, Holland, 112 pp.

Song, H., Marshall, J., Follows, M. J., Dutkiewicz, S., & Forget, G. (2016). Source waters for the highly productive Patagonian shelf in the southwestern Atlantic. Journal of Marine Systems, 158, 120-128. http://doi.org/10.1016/j.jmarsys.2016.02.009.

St. Laurent, L. and Schmitt, R. W. (1998). The Contribution of Salt Fingers to Vertical Mixing in the North Atlantic Tracer Release Experiment. *Journal of Physical*

Oceanography, 29(7), 1404-1424. http://doi.org/10.1175/1520-0485(1999)029<1404:TCOSFT>2.0.CO;2

Suggett, D. J., Moore, C. M., Hickman, A. E. and Geider, R. J., 2009. Interpretation of fast repetition rate (FRR) fluorescence: Signatures of phytoplankton community structure versus physiological state. *Marine Ecology Progress Series*, 376, 1-19. http://doi.org/10.3354/meps07830.

Suggett, D., Kraay, G., Holligan, P., Davey, M., Aiken, J., and Geider, R., 2001. Assessment of photosynthesis in a spring cyanobacterial bloom by use of a fast repetition rate fluorometer. *Limnology and Oceanography*, 46(4), 802-810.

Sun, J. and Liu, D., 2003. Geometric models for calculating cell biovolume and surface area for phytoplankton. *Journal of Plankton Research*, 25(11), 1331-1346. http://doi.org/10.1093/plankt/fbg096.

Tarran, G. A., Heywood, J. L. and Zubkov, M. V., 2006. Latitudinal changes in the standing stocks of nano- and picoeukaryotic phytoplankton in the Atlantic Ocean. *Deep-Sea Research Part II: Topical Studies in Oceanography*, 53(14-16), 1516-1529. http://doi.org/10.1016/j.dsr2.2006.05.004.

Thorpe, S. A., 2007. An Introduction to Ocean Turbulence. Cambridge University Press, NY, 293 pp.

Tomas, C. R., 1997. Identifying Marine Phytoplankton. Academic press., California, USA, 875 pp.

Tonini, M., Palma, E., & Rivas, A., 2006. Modelos de alta resolución de los golfos patagónicos. *Mecánica Computacional*, XXV, 1441-1460.

Tremblay, G., Belzile, C., Gosselin, M., Poulin, M., Roy, S., and Tremblay, J. É., 2009. Late summer phytoplankton distribution along a 3500 km transect in Canadian Arctic waters: Strong numerical dominance by picoeukaryotes. *Aquatic Microbial Ecology*, 54(1), 55-70. http://doi.org/10.3354/ame01257.

Utermöhl, H., 1958. Zur Vervollkommnung der quantitativen Phytoplankton-Methodik: Mit 1 Tabelle und 15 abbildungen im Text und auf 1 Tafel. *Internationale Vereinigung für Theoretische und Angewandte Limnologie: Mitteilungen,* 9(1), 1-38.

Valiadi, M., Painter, S. C., Allen, J. T., Balch, W. M., and Iglesias-Rodriguez, M. D., 2014. Molecular detection of bioluminescent dinoflagellates in surface waters of the Patagonian shelf during early austral summer 2008. *PloS one*, 9(2), e98849. http://doi.org/10.1371/journal.pone.0098849.

Veldhuis, M. J. W., Timmermans, K. R., Croot, P., and Van Der Wagt, B., 2005. Picophytoplankton; A comparative study of their biochemical composition and photosynthetic properties. *Journal of Sea Research*, 53(1-2 SPEC. ISS.), 7-24. http://doi.org/10.1016/j.seares.2004.01.006.

Verity, P. G., and Langdon, C., 1984. Relationships between lorica volume, carbon, nitrogen, and ATP content of tintinids in Narrangasett Bay. *Journal of Plankton Research*, 6(5), 859-868.

Vidal, M., Duarte, C. M., and Agusti, S., 1999. Dissolved organic nitrogen and phosphorus pools and fluxes in the central Atlantic Ocean. *Limnology and Oceanography*, 44(1), 106-115. http://doi.org/10.4319/lo.1999.44.1.0106.

Williams, G. N., Dogliotti, A. I., Zaidman, P., Solis, M., Narvarte, M. A., González, R. C., Gagliardini, D. A., 2013. Assessment of remotely-sensed sea-surface temperature and chlorophyll-a concentration in San Matías Gulf (Patagonia, Argentina). *Continental Shelf Research*, 52:159- 171, https://doi.org/10.1016/j.cs r.2012.08.014.

Yentsch, C. S., Yentsch, C. M., Phinney, D. A., Lapointe, B. E., & Yentsch, S. F. W., 2004. The odyssey of new production. Journal of Experimental Marine Biology and Ecology, 300(1-2), 15-30. http://doi.org/10.1016/j.jembe.2003.12.025.

Yorio, P., 2009. Marine protected areas, spatial scales, and governance: implications for the conservation of breeding seabirds. *Conservation Letters*, 2(4), 171-178. http://doi.org/10.1111/j.1755-263X.2009.00062.x.

Yorio, P., Frere, E., Gandini, P., and Schiavini, A., 2001. Tourism and recreation at seabird breeding sites in Patagonia, Argentina: Current concerns and prospects. Bird Conservation International, 11(4), 231-245. http://doi.org/10.1017/S095927 0901000314.

Zhang, J., Schmitt, R. W., and Huang, R. X., 1998. Sensitivity of the GFDL Modular Ocean Model to Parameterization of Double-Diffusive Processes. *Journal of Physical Oceanography*, 28(4), 589-605. http://doi.org/10.1175/1520-0485(1998)028<0589:SOTGMO>2.0.CO;2.

Zubkov, M. V., Sleigh, M. A., Burkill, P. H., and Leakey, R. J. G., 2000. Picoplankton community structure on the Atlantic Meridional Transect: A comparison between seasons. Progress in Oceanography, 45(3-4), 369-386. http://doi.org/10.1016/S00 79-6611(00)00008-2.

Zuur, A. F., Ieno, E. N., and Elphick, C. S., 2010. A protocol for data exploration to avoid common statistical problems. Methods in Ecology and Evolution, 1(1), 3-14. http://doi.org/10.1111/j.2041-210X.2009.00001.x.

ANNEXES

ANNEXE I: Richardson number estimate at different water column depth, for all stations using ADC and CTD data. The yellow boxes correspond to the depth of maximum N^2

	Station						
	G01	G02	G03	G04	G05	G06	G07
Depth	Richardson number						
12.13	1.397512	0.397172	0.009174	0.115042	0.006481	0.024204	0.016394
16.13	0.753418	0.708092	0.26525	0.259085	0.087573	0.099182	0.087839
20.13	0.612119	0.356995	0.9237	0.521402	0.72561	0.14089	0.353796
24.13	2.201077	0.188698	1.825338	0.218064	0.08928	0.44809	0.391822
28.13	1699.032	0.637871	4.156582	0.304451	0.208129	0.251255	0.849188
32.13	10.8978	2.387011	10.43155	2.141509	2.95739	7.832236	1.05675
36.13	5.425656	5.436257	23.86723	0.653668	0.521591	17.37953	1.046751
40.13	4.733541	138.0167	5.490708	2.451372	0.152049	11.43355	9.523781
44.13	6.106545	1.196076	8.90815	3.795604	0.052747	33.40688	41.48257
48.13	5.206886	0.602066	14.35228	1.456977	0.294536	3.576438	6.518356
52.13	13.20904	0.090623	3.28646	2.6078	2.716706	4.09134	1.022811
56.13	132.6333	0.01497	0.998519	1.68338	0.125993	5.652206	2.466416
60.13	21.24304	0.035108	0.842795	5.692943	4.000693	1.123528	1.744424
64.13	0.936394	0.067039	0.569533	1.478839	NO DATA	0.865406	17.5426
68.13	1.572926	0.018604	3.818444	4.776744	NO DATA	0.808844	6.528484
72.15							1.245771
76.15							0.449826

Depth	Station						
	G08	G09	G10	G11	G12	G13	G14
	Richardson number						
12.13	0.015188	3.044026	0.004021	2.95E-05	0.416673	1.775852	0.059922
16.13	0.026723	1.649665	0.017026	0.343942	0.85851	0.227705	1.66863
20.13	0.30692	0.539849	-0.02894	0.415366	6.904565	0.149606	0.413283
24.13	0.42151	0.588369	0.009015	0.116758	0.216116	1.936599	0.132435
28.13	1.451886	11.05156	0.807848	-0.0033	0.107111	27.61272	0.321115
32.13	4.206772	4.099946		0.473663	0.214579	1.590585	0.534622
36.13	26.34058	2.035025		0.281918	0.246546	0.791801	6.295396
40.13	5.665928	0.807848		0.540148	0.091591	0.579386	3.797618
44.13	27.62461	1.756569		4.352849	0.029746	0.312959	2.136255
48.13	1.974529	1.34365		2.233233	0.448799	0.83878	0.209704
52.13	0.673061	4.194258		0.365361	0.400099	0.272194	0.492313
56.13	318.4088	1.013119		0.190189	2.143251	0.885114	0.46842
60.13	0.494522	1.429534		0.482133	-0.87368	0.302947	0.199718
64.13	4.28644	7.965116		7.979602	0.082293	0.241812	0.571449
68.13	0.778609			42.54358		0.025695	9.201601
72.13	2.811498						0.808906
76.13	5.049549						
80.13	2.123847						

71

	Station					
	SF10	SF11	SF12	SF13	SF14	SF15
Depth	Richardson number					
12.13	0.041299	0.05954	0.04351	0.008373	0.008621	1.85258
16.13	0.055359	0.079239	2.024487	0.12669	0.159373	3.036105
20.13	0.197107	0.816545	0.04681	0.779932	35.85716	0.690916
24.13	0.457943	0.095935	0.054676	0.129788	0.396793	19.20354
28.13	2.999213	1.35916	0.247127	0.112525	0.322941	5.050976
32.13	3.145474	41.09518	0.661745	9.949575	0.614458	0.42928
36.13	5.232285	1.968415	2.946298	0.734991	1.161726	3.819025
40.13	1.151671	0.325333	0.879946	0.335526	1.874909	2.05423
44.13	3.91004	0.735579	0.466805	0.500264	3.733755	0.610546
48.13	3.188818	11.24186	2.164942	0.605339	0.305571	2.507087
52.13	1.190412	12.07564	0.287449	0.014516	0.2475	40.09289
56.13	3.073897	0.278363	1.059101	0.362339	7.14377	4.697006
60.13	0.364448	0.381481	1.278526	0.004315	0.768277	4.469335
64.13	0.409856	4.23552	0.733313	0.067989	3.722294	5.647596
68.13	5.987347	2.590682	0.417559	0.068021	1.452879	1.408304
		0.04813	0.808534		0.342966	

	Station						
	SF01	SF02	SF03	SF04	SF06	SF08	SF09
Depth	Richardson number						
12.13	0.015224	0.015224	0.600881	0.008944	0.016634	-0.00041	0.076988
16.13	0.285783	0.285783	0.110166	-0.08679	0.361319	0.008935	0.126206
20.13	0.418465	0.418465	0.070971	2.153531	0.074976	3.76859	0.078321
24.13	0.034513	0.034513	0.767054	2.407929	8.156365	0.57554	0.046634
28.13	0.153822	0.153822	0.264606	196.5864	13.52212	0.362857	0.112232
32.13	1.580499	1.580499	0.220858	0.38381	11.97049	2.273989	2.455723
36.13	1.759298	1.759298	17.57239	3.924769	3.09792	3.171953	4.086335
40.13	0.498932	0.498932	0.843556	0.698598	0.152737	1.367576	2.454764
44.13	1.185805	1.185805	1.439837	0.383155	0.016811	1.77979	2.233395
48.13	14.92899	14.92899	0.745916	0.287559	0.026257	1.264936	0.904311
52.13	0.154145	0.154145	0.499908	0.167901	0.198585	16.57857	2.971974
56.13	0.089884	0.089884	7.498591	0.322417	0.274595	3.712768	3.660652
60.13	4.555965	4.555965	0.26966	0.846625	0.935799	1.143656	0.958339
64.13	1.282473	1.282473	30.76663	0.109388	0.234995	0.834962	0.436708
68.13	1.263395	1.263395	2.938113	0.261487	0.366642	0.15927	12.32423
72.13	0.966148	0.966148		6.306625	0.344559	0.325188	

ANNEXE II: Density Ratio estimate at different water column depth CTD data.

Depth	G01	G02	G03	G04	G05	G06	G07
				Rp			
2	-1.14761	-1.71846	999	NaN	-999	NaN	999
3	0	-1.71953	999	999	999	NaN	999
4	999	-0.86003	999	999	999	999	-999
5	999	-0.57333	-999	-999	-1.39223	2.285307	-999
6	999	-1.62494	-999	-999	0.557046	-999	999
7	-999	-1.43253	999	0	-999	-999	6.488316
8	-999	-1.19187	999	NaN	3.897147	-999	15.88996
9	999	-1.35964	999	-999	0.835018	-999	-999
10	-999	-0.85902	-0.85744	2.691519	-999	0.856418	-999
11	-27.8016	-1.39074	-3.14371	3.208323	0.742315	3.995673	-999
12	-11.299	-1.62467	-1.71429	4.349743	1.253221	-999	-3.21594
13	-8.05621	-1.87306	-0.28568	3.554692	2.042584	-999	-999
14	-8.37127	-4.83101	0	4.47143	2.50425	-999	-999
15	-999	-3.40951	-1.96442	5.434372	-999	-999	-999
16	5.454587	-2.55658	-1.79625	13.98244	4.589645	NaN	-3.21455
17	3.480473	-999	-1.49616	10.05143	5.001114	-999	-2.33757
18	3.292865	-999	-0.96865	8.153483	5.827134	2.996006	-999
19	4.424489	-3.12388	-0.96842	31.10361	6.649039	2.94624	-999
20	8.166884	-2.5557	-1.32881	18.30381	5.261094	3.134719	-999
21	12.78489	-999	-1.01226	11.07524	9.957308	2.989711	4.08826
22	13.58299	-999	-0.83541	8.013069	-0.82943	3.129149	4.379081
23	17.59837	-4.25642	-1.1178	6.351817	-0.46075	3.40498	-999
24	-999	-4.82267	-7.84934	8.00579	-0.48371	4.057341	6.127482
25	-1.80885	-7.08991	3.76186	5.61919	-0.62196	5.935854	7.582643
26	-3.25713	-8.78553	5.509291	4.395847	-0.48362	13.54998	7.870455
27	-32.0808	10.76294	11.26622	7.397737	0.138201	-7.05207	3.884541
28	-34.5891	10.75242	6.777802	18.70034	0.046076	-4.08931	6.40253
29	-21.1718	7.069737	3.130844	11.36556	-0.06912	-8.73427	8.28007
30	-14.6556	5.088291	3.774867	11.17124	-0.27651	-999	6.822496
31	-6.33534	-999	7.744001	13.50371	-1.29019	8.616714	11.74311
32	6.133018	5.839182	37.24389	20.83786	-1.77566	9.013241	8.390121
33	2.544987	6.200174	31.04697	-999	-1.47168	27.54029	6.716168
34	4.527112	7.747335	13.57695	-999	-0.48274	-10.7399	8.356262
35	12.73587	6.846723	11.81891	-13.5882	0.137958	6.687932	7.759448
36	-6.64982	3.108155	46.60192	-14.3678	-0.82784	5.450131	7.790577
37	-6.46784	2.754958	-6.29269	-999	-0.87368	5.40685	5.991264

38	-3.70001	3.949853	-1.47815	-27.0225	-0.55151	5.097201	5.439632
39	-2.92169	-9.53756	-2.15834	34.76454	-0.6617	5.70317	6.46954
40	-2.44228	-5.38961	-2.86906	41.72478	11.85374	5.3202	6.127852
41	-3.74171	-13.1717	-2.1905	199.7829	6.879804	10.27406	5.651049
42	-3.4811	62.36506	-1.38166	-169.398	4.675771	15.54602	6.249801
43	-3.19107	11.18406	-0.46962	-65.9459	3.575092	6.743198	14.52684
44	-3.92095	-63.2732	-0.88417	-37.9514	2.749262	9.731179	17.76298
45	-4.19798	-5.8217	-3.02434	-21.9435	2.610529	57.30731	10.6339
46	-3.64967	-1.95692	-6.3493	-9.64753	1.923074	-17.1157	-999
47	-3.23817	-1.82017	-13.0573	-2.76401	2.334585	-17.4205	-6.33165
48	-2.94524	-2.2496	-11.0447	-2.08434	5.765545	-62.8071	-13.3094
49	-3.88432	-2.15011	-4.21912	-1.90254	3.841868	-999	-4.91829
50	-7.41335	-3.30185	-2.41292	-1.7688	2.399394	-13.3314	-0.87527
51	-5.13707	-5.72379	-3.38612	-2.03715	2.082404	-10.4348	-0.66929
52	-5.43212	-3.33199	-3.48424	-1.68871	1.672948	-7.72193	-1.62892
53	-3.13769	-2.40623	-3.48145	-1.44757	2.049767	-7.2874	-0.82001
54	-1.70489	-3.34317	-999	-1.04114	-999	-12.4754	-0.29285
55	-1.21852	-4.65721	-999	-1.40904	4.097791	-5.75209	-0.85901
56	-3.52376	-4.81914	-3.88903	-2.59777	-999	-3.39996	-1.209
57	-10.7768	-9.75448	-999	-3.67763	-999	-2.09494	-1.03928
58	-8.08539	-7.49613	2.454075	-2.28589	11.04589	-3.03921	-0.77937
59	-4.93938	-12.6134	-999	-2.76698	11.06117	-2.83604	-0.58442
60	-3.28715	-999	-999	-5.69278	9.310214	-10.1233	-0.71417
61	-2.92514	-29.3716	-999	-6.80122	6.586544	-999	-0.84379
62	-2.90892	6.009119	7.33396	-10.3821	7.701788	-17.5307	-0.84352
63	-2.83766	3.238881	-999	-15.8544	9.190174	-18.0678	-1.16765
64	-2.45683	15.46175	-999	-8.84107	6.396661	-999	-1.16734
65	-3.5551	-12.4175	9.106184	-26.3494	5.932145	-999	-1.36096
66	-4.94404	-9.38349	8.523784	-17.4316	9.530422	-999	-1.3603
67	-4.32975	-3.18729	28.19977	-10.8037	50.23917	-999	-0.89323
68	-4.18201	-1.12495	-999	-7.41587	-999	-999	-1.0997
69	-3.837	-999	-999	-7.12802	-194.96	-32.2389	-3.10041
70	-3.54839	2.06151	-1.38075	-4.19905	-16.9572	-10.9742	-2.83723
71	-3.22591	-999	-0.39451	-3.95554	-4.25224	-10.3796	-1.2559
72	-2.71491	-1.68557	0	-8.30988	-0.0005	-4.8815	-1.22214
73	-1.90879	-0.56188	NaN	-11.1274	-0.0005	-1.75662	-1.19498
74	-0.80361	-1.12386	NaN	-999	-0.0005	NaN	-1.28393
75	-1.70749	-0.93636	NaN	-9.47094	-0.0015	-999	-1.05888
76	-3.41241	-0.79546	-999	-3.02038	-0.002	-999	-1.34751
77	-4.87799	-0.84197	0.394833	-999	-0.001	-999	-0.96245

78 -4.44468	-999	0.19743	-999	0	-999	-0.96249
79 NaN	-999		-999	0	NaN	-999
80 NaN	-999		0.805366	0	0	-999

	G08	G09	G10	G11	G12	G13	G14
Depth				Rp			
2	NaN	NaN	-999	NaN	2.781158	NaN	4.159444
3	NaN	999	0.272718	999	-999	NaN	-999
4	-0.58294	0.850775	999	999	8.088154	-0.13677	-0.59382
5	0.874568	0.945168	-0.54565	-999	-999	-0.18242	999
6	0	1.98445	999	-999	-999	-9.85003	14.56452
7	999	0	-999	-999	999	-2.32228	9.524853
8	999	0.567101	-999	999	999	-0.09108	NaN
9	-0.87505	0.708692	-999	999	0.505688	-0.13662	-999
10	0.875126	0	-999	-999	-999	-0.27327	2.38185
11	-999	1.360935	-999	999	10.87011	-0.81985	5.655381
12	-999	2.053106	-999	999	16.2774	-0.54657	11.79243
13	-999	1.41589	-999	-999	13.47503	-0.51739	14.01763
14	-999	1.822073	-999	-999	21.52008	-0.62025	29.54861
15	-999	1.959499	-999	-999	-999	-4.22881	-10.3217
16	1.458245	1.996005	-999	-7.18029	-999	4.633517	8.852698
17	1.166692	2.255617	-999	-4.86706	-999	4.518262	9.746099
18	-999	2.773815	-999	-2.90108	-999	4.886786	-999
19	3.49994	2.216541	999	999	-999	6.504789	-7.36211
20	2.332343	3.227908	999	-7.30043	-999	-14.8819	-999
21	4.568534	2.844679	999	-3.57073	-999	-4.14556	-999
22	6.5952	2.435743	999	-5.22549	-999	-25.3821	-999
23	5.524401	2.681568	999	-7.12778	-999	6.298374	-999
24	4.94307	3.032302	-999	-2.88105	12.86642	4.133513	-999
25	-8.42705	2.682964	-999	-999	-999	3.792044	-999
26	-4.35674	2.796869	-999	1.017017	-9.35348	3.672262	-999
27	-999	3.704683	-999	999	-11.316	4.706726	5.296651
28	-999	1.621383	-999	-3.81791	-999	9.442378	7.058734
29	-999	2.622825	-999	-999	-6.62594	16.7802	4.703766
30	11.3155	3.71002	-999	-2.80028	-7.35822	-6.70444	3.233389
31	5.604584	-12.5153	-999	-4.40779	-999	-1.54713	-999
32	6.309627	64.34038	-999	-5.06462	-3.43008	-0.87667	7.05067
33	7.039748	17.95821	NaN	-3.9216	-4.89831	-0.30455	6.459936
34	5.411987	25.61472	NaN	-5.05753	-999	-0.03515	6.256127

35	5.401131	9.643969	NaN	-2.52797	-999	-2.33166	5.798162
36	6.317861	6.237193	46.60192	-1.64236	-999	-23.681	5.612873
37	6.040132	6.103299	-6.29269	-999	-2.93613	14.86426	6.259511
38	4.779486	6.017409	-1.47815	-4.04321	-3.66902	11.40276	6.521781
39	7.942231	3.324827	-2.15834	-5.30285	-999	13.64224	8.460564
40	7.119923	2.911511	-2.86906	-3.47645	-999	9.107744	12.07856
41	6.934381	5.739342	-2.1905	-1.3212	-999	3.903881	-999
42	6.981149	-56.1303	-1.38166	-0.62926	-999	8.485006	-4.84715
43	6.873493	-5.7939	-0.46962	-2.68417	-999	7.929357	13.96615
44	7.409929	-2.14553	-0.88417	-2.26192	-999	14.73573	19.34773
45	9.399708	-1.91115	-3.02434	-3.77014	-999	-13.0778	12.50365
46	-6.40269	-2.04794	-6.3493	-7.0331	-3.66271	-12.739	4.934913
47	-2.91854	-4.02982	-13.0573	-4.57435	-999	-10.6269	5.891556
48	-1.73577	-999	-11.0447	-4.20423	-999	-22.855	6.072236
49	-1.38089	-11.4029	-4.21912	-4.10013	-5.9723	-19.5246	8.152209
50	-0.47581	-3.85811	-2.41292	-3.51838	-9.01202	-5.05061	15.32098
51	-0.75457	-3.6864	-3.38612	-3.10373	-5.10982	-3.13242	12.94956
52	-1.19344	-2.3286	-3.48424	-2.97785	-1.70331	-2.22906	7.442117
53	-0.31555	-2.51914	-3.48145	-1.90162	-999	-1.29399	11.31429
54	0.024273	-2.68414	-999	-4.33842	-999	-1.07807	259.7229
55	0.138777	-2.3016	-999	-4.82872	999	-1.07789	-29.7383
56	0.123673	-1.63443	-3.88903	-2.22688	-999	-0.96988	-2.76495
57	-0.30055	-1.75394	-999	-999	-999	-0.80775	-2.4859
58	-1.05415	-2.01371	2.454075	999	NaN	-1.72313	-1.70215
59	-1.16409	9.545534	-999	-999	999	-1.72282	-0.63245
60	-1.66627	8.192306	-999	-999	999	-0.53836	-0.08519
61	-1.8795	-999	-999	-3.83533	999	-1.07675	-0.03976
62	-1.31788	-1.35117	7.33396	-3.33653	999	-999	-0.14913
63	-0.90697	-1.17322	-999	-3.67553	-999	-0.21535	-0.26511
64	-0.90518	-1.35659	-999	-3.12481	-999	-0.21537	-0.29828
65	-1.40799	-1.41724	9.106184	-2.69781	-1.94804	-999	-0.99431
66	-2.20528	-1.45565	8.523784	-2.36853	-4.86883	-999	0.795398
67	-7.84794	-1.44515	28.19977	-1.60098	-999	-0.53853	-0.19898
68	7.075861	-1.52957	-999	-1.9403	-999	-0.37696	-1.59121
69	-9.73718	-1.42273	-999	-1.37364	-999	-0.40665	0
70	-11.0523	-1.39374	-1.38075	NaN	-999	-0.37668	0.397936
71	-999	-1.2363	-0.39451	NaN	-999	-0.43053	1.591624
72	-3.6119	-1.13143	0	-8.30988	999	-999	-999
73	-5.69843	-1.26734	NaN	-11.1274	999	NaN	-999
74	-4.55361	-1.09478	NaN	-999	999	NaN	-999

Depth							
75	-4.63845	-0.82057	NaN	-9.47094	-999	NaN	-999
76	-4.9165	-0.79546	-999	-3.02038	-6.81729	0	-999
77	-4.34703	-0.84197	0.394833	-999	NaN	0	0.795422
78	-7.55266	-999	0.19743	-999	NaN	NaN	0.397739
79	-3.1415	-999		-999	NaN	NaN	-999
80	-5.08051	-999		0.805366	0	NaN	-999

	SF01	SF02	SF03	SF04	SF06	SF07	SF08
Depth				Rp			
2	1.921785	999	NaN	NaN	NaN	-0.1338	NaN
3	-999	4.894031	NaN	NaN	NaN	0.267631	NaN
4	1.92171	999	-999	-999	-1.33675	0	NaN
5	1.098441	1.631915	NaN	999	-999	0.267696	-999
6	3.293681	1.631684	0	999	1.069413	0.535389	999
7	-999	2.084385	999	999	-999	1.606255	-999
8	999	-999	-0.26652	-999	-0.26738	2.007507	-999
9	1.921247	-3.53012	-999	-999	999	1.337797	NaN
10	3.293069	-999	0.799674	999	999	1.605506	-999
11	-0.54869	1.086254	-999	-999	NaN	-0.26753	-999
12	1.234985	2.444056	5.86463	-999	-0.26752	1.33815	-999
13	1.098098	2.443471	-999	-999	0	999	-999
14	1.006691	1.69608	-999	999	-1.0703	999	999
15	1.748478	2.531284	-999	-999	-999	999	999
16	2.519614	1.965004	-999	-999	4.011854	999	999
17	0.455337	1.625129	-999	999	-999	NaN	-999
18	1.457753	1.691735	-999	999	999	-999	3.481421
19	1.456127	1.623401	-999	999	999	NaN	3.48088
20	1.659058	1.48767	-999	-999	-999	999	8.827249
21	2.060011	1.554331	-999	-999	-999	999	-999
22	2.992602	1.686917	0.531312	-999	2.407904	1.071851	2.940838
23	1.631011	1.618119	0.797043	-999	3.922406	1.250823	4.810813
24	1.630187	1.526976	-999	-999	8.009794	999	-999
25	1.249179	1.686127	-999	-999	3.872815	1.74284	5.341679
26	1.809557	1.611354	4.51325	6.411605	4.05899	2.811195	2.802967
27	1.985823	1.340502	5.042923	5.337056	3.432649	1.3395	9.072598
28	1.623445	1.473559	-999	-999	4.045704	1.60707	-999
29	1.687565	1.516963	2.121973	4.800767	4.177708	2.767884	-999
30	1.817468	1.490944	1.856622	3.997021	4.774277	2.781789	6.125813
31	2.094037	1.600964	-999	3.859086	7.71128	2.939299	4.852839
32	2.71407	2.57787	-999	3.720355	4.684081	2.271514	3.397266

33	2.810295	2.26515	-999	2.656314	5.146208	1.655935	3.728369
34	2.723647	1.577123	3.975563	2.652506	7.159924	2.855124	3.055026
35	3.447313	2.155065	4.768726	2.280224	9.464329	4.415228	3.710509
36	3.701142	2.697076	5.689065	3.917829	-30.7994	8.573249	5.488681
37	4.213166	3.404395	6.463418	5.474149	-3.65427	9.365679	11.01255
38	3.278044	4.894261	11.5575	5.317658	-2.41947	6.058733	14.16555
39	5.286111	18.72069	6.145393	5.265653	-2.07367	9.310011	12.13902
40	8.040313	14.16046	5.437228	6.244639	-1.63299	145.0276	6.484499
41	7.297182	7.113392	10.62781	5.956773	-4.20128	20.22152	10.87422
42	6.986774	6.654453	5.101932	5.599153	-6.73596	23.58279	-7.26365
43	7.466947	5.642635	5.848896	6.941365	-2.57946	-39.4496	-1.71421
44	14.04813	7.774862	8.213465	8.728609	-0.89712	-1.78579	-1.31875
45	-17.1817	5.310628	4.508311	7.390807	-2.24243	-0.55785	-1.48554
46	-1.44284	6.199834	7.025022	7.340603	-999	-0.50197	-1.34282
47	-0.45402	18.70876	21.30846	9.525891	-5.3766	-0.59491	-0.50358
48	-0.29706	18.31331	14.50636	14.24121	-3.80668	-0.74352	-1.26794
49	-0.26136	20.85571	-2.58148	-999	-3.35783	-2.23007	-3.13109
50	-0.34221	-1.06451	-2.48527	-18.583	-3.58044	-2.89858	-2.3088
51	-0.52256	-0.49294	-2.02914	20.23163	-3.20631	-4.45068	-2.00946
52	-0.50791	-0.72806	-2.25267	-18.1468	-2.73463	-11.5545	-2.89887
53	-1.21237	-1.34366	-2.06857	-3.56384	-2.14151	-4.43745	-2.61791
54	-1.04256	-1.64088	-1.01111	-2.10965	-2.078	-4.21251	-2.5577
55	-0.3798	-1.78965	-0.98796	-1.46863	-2.27933	-3.32486	-2.61865
56	-0.33386	-2.45961	-1.19712	-1.12953	-1.85121	-3.32328	-1.7732
57	-0.72279	-2.79334	-1.57068	-3.27512	-2.22082	-2.21512	-1.4102
58	-1.53542	-2.34471	-2.46663	-7.78219	-1.55439	-1.54938	-1.48117
59	-2.01451	-1.89744	-3.08886	-6.67438	-1.4063	-0.88516	-1.62522
60	-0.20277	-1.94447	-2.6801	-3.36585	-1.63623	-6.41757	-1.16274
61	0.298688	-1.78651	-1.78589	-5.82932	-1.54918	-17.8969	-1.1347
62	0.302518	-1.58413	-1.89708	-999	-1.32757	-1.4314	-1.16632
63	0.195645	-1.24804	-2.78833	-3.46985	-999	-0.39884	-1.15544
64	0.367995	-1.14904	-2.61913	-2.46101	-0.88518	-0.74447	-1.10938
65	0.567094	-1.78621	-1.83539	-1.90079	-0.73762	-1.12233	-1.08922
66	-1.01846	-1.4031	-1.54053	-2.90626	-0.95864	-1.26607	-1.26991
67	-2.26883	-1.02568	-1.33789	-2.12317	-1.43764	-1.29887	-1.1493
68	-5.6746	-0.8544	-1.16977	-1.34008	-1.45818	-1.17818	-1.08625
69	13.2015	-0.55952	-1.4249	-4.68953	-1.39826	-1.42924	-1.30329
70	2.669739	0	-1.34448	-4.46237	-1.44532	-1.53123	-1.52005
71	3.041578	0.223353	-1.09342	-1.83827	-1.34027	-1.59035	-1.51828
72	-5.96655	-0.56203	-1.00456	-1.11366	-1.24459	-1.50421	-1.40818

73	-1.34504	-2.75312	-1.10885	-1.41023	-0.98843	-1.39671	-1.23667
74	-1.21128	-5.34114	-1.17278	-1.78019	-0.98803	-1.32059	-1.35095
75	-1.39439	-4.58251	-1.15219	-1.81613	-1.37162	-1.33653	-1.40272
76	-1.50237	-5.80375	-1.36419	-1.56969	-1.38881	-1.81585	-1.25714
77	-1.32674	-3.4394	-1.312	-1.57834	-1.21671	-1.40872	-1.32974

	SF09	SF10	SF12	SF13	SF14	SF15
Depth				Rp		
2	999	5.696493	999	-999	-999	-999
3	-9.24537	17.65209	1.074242	-999	-0.26866	999
4	-3.80967	6.078707	1.611113	0.267409	-999	999
5	13.88018	21.52926	NaN	-999	1.746597	999
6	21.71867	-6.55883	2.685746	1.069807	3.491618	999
7	7.863067	-999	2.955976	-999	-999	-999
8	5.054268	10.7087	999	2.138359	2.685886	18.39739
9	13.25178	13.53192	3.494151	4.818386	2.953433	-999
10	5.673512	13.64101	2.14917	3.478713	-999	-13.1916
11	3.50918	7.880535	-999	-999	999	-6.42216
12	5.393662	23.86162	2.149298	2.675827	999	-4.12575
13	5.38885	-999	3.938944	2.764042	-999	-3.47932
14	9.152862	-999	4.251684	3.117533	4.028704	-6.85367
15	-999	-999	4.340751	5.341115	5.230485	-18.2656
16	4.572414	-999	9.072448	-999	-999	-999
17	4.570805	-2.93639	-8.81389	2.535665	-999	18.45749
18	4.300468	-2.13549	-0.63424	3.720228	-999	36.35834
19	4.299165	-999	-0.79299	0.530904	10.98512	-999
20	-999	-999	-2.9066	2.437195	7.090583	-56.8383
21	-999	-999	-0.13211	3.514043	8.552372	37.20525
22	3.223307	-2.66808	0	10.02965	-999	66.14022
23	4.56429	-2.13418	-999	-999	6.678285	-13.6304
24	-999	-999	-3.17066	-0.08775	10.94305	-32.3839
25	-999	-2.9338	-1.32093	0.438869	8.932403	-50.698
26	-2.14751	-1.20003	2.37781	0.579602	5.480873	38.62346
27	-3.22084	-3.19966	4.423776	-999	6.809232	43.16849
28	-999	-3.86512	4.60864	5.794032	4.638719	-999
29	-2.14661	18.90835	3.80976	7.898594	3.739449	15.33778
30	-4.02436	5.047689	4.165587	8.416569	4.103306	15.08497
31	7.777009	3.335981	4.610662	4.995336	4.129433	20.06175
32	3.006941	3.507642	4.741223	3.085084	4.074755	17.8841
33	2.735298	5.510202	4.821495	4.942738	4.551213	14.70097
34	2.850388	5.982417	4.854154	5.610947	4.7093	-4.20942

35	3.048048	9.773007	6.174199	3.955675	4.684097	-2.19893
36	3.450965	19.12732	13.48682	4.180154	4.963274	-5.9073
37	7.075221	-15.8587	-42.0651	4.389657	6.419771	-1.0223
38	9.368822	-10.2765	-6.14185	5.942712	9.40137	-1.02209
39	6.08923	-10.4774	10.35299	7.180444	7.106007	-2.57253
40	10.80268	-5.87302	12.40967	4.526882	8.882599	-9.52265
41	16.70365	-3.13078	21.56389	7.844084	17.84174	-10.644
42	22.98703	-2.73616	31.25762	10.65918	5.610838	-4.86203
43	-36.2171	-10.0526	12.86658	7.830842	5.351642	-8.35983
44	-999	-4.79047	18.89673	-64.4262	11.36318	-999
45	-999	-1.40428	-33.0686	-7.03272	-12.4453	-4.05953
46	-10.0047	-1.41828	-7.35797	-5.54382	-3.25831	-1.80394
47	-3.80545	-1.03784	-4.97105	-2.74933	-2.08472	-999
48	-2.69183	-0.80956	-3.28695	-1.79313	-1.71652	-3.38142
49	-2.37809	-0.55739	-2.34913	-1.31049	-1.34185	-5.18274
50	-1.91517	-0.37919	-2.54644	-0.55914	-1.11817	-999
51	-1.18655	0.067705	-4.42724	-0.44733	-1.11778	-999
52	-0.60267	0.136957	-4.6455	-0.89462	-1.6766	4.271754
53	-0.53518	-0.01669	-5.96276	-2.01257	-2.45755	3.371172
54	-1.77511	-0.49586	-2.48444	-1.78875	-1.89811	8.529698
55	-1.4511	-1.85294	-1.31886	-4.02428	-1.5627	-999
56	-0.24467	-6.90992	-1.53633	-3.90961	0	-14.5427
57	0.391964	-0.27459	-1.72478	-2.06414	-0.44661	-4.58037
58	0.499675	0.359727	-1.96801	-1.41202	-999	-4.2411
59	0.412141	0.586181	-1.78303	-0.89177	-3.12578	-7.35757
60	0.357552	0.778198	-1.36289	999	-999	-5.79331
61	0.116128	0.732323	-0.87222	999	-15.3848	-6.45709
62	0.087145	0.394936	-0.76306	-0.44607	-2.97838	-5.00579
63	0.043584	-0.02179	0.345665	-1.11526	-0.48124	-10.1055
64	-0.10899	-0.05449	0.413299	-3.56737	0.148101	-999
65	-0.76281	-0.10899	-0.07302	-2.44926	-1.25911	-2.75885
66	-1.5606	-0.6228	-0.36472	-1.66806	-1.40022	-1.04274
67	-4.23977	16.98666	-0.07295	-1.53628	-1.36096	-0.85293
68	3.911037	7.88229	5.034257	-1.54946	-1.43624	-0.83416
69	-15.7111	9.300357	1.894477	-1.5914	-1.46334	-1.19488
70	-5.04418	15.64392	3.272914	-1.37154	-1.43024	-2.70347
71	-4.93321	57.6484	3.267022	-1.10169	-1.29617	-8.4931
72	9.03428	-31.278	2.466306	-1.32212	-1.19393	-2.32042
73	-8.60298	-5.46533	4.67329	-1.26683	-1.09541	-0.08696
74	-2.55445	-2.63235	-12.155	-1.22623	-0.98589	-0.33472

75	-2.98247	-2.51295	-1.91367	-1.37402	-1.44477	-10.643
76	-2.79529	-2.7374	-1.08196	-1.86845	-1.44344	-0.89182
77	-2.60435	-2.82278	-1.4704	-1.29058	-1.48594	-0.34873

ANNEXE III: Nitrate vs. phosphate regression.

ANNEXE 4 : F_v/F_m vs. σ_{PSII}